

# We are IntechOpen, the world's leading publisher of Open Access books Built by scientists, for scientists

6,900

Open access books available

185,000

International authors and editors

200M

Downloads

Our authors are among the

154

Countries delivered to

TOP 1%

most cited scientists

12.2%

Contributors from top 500 universities



WEB OF SCIENCE™

Selection of our books indexed in the Book Citation Index  
in Web of Science™ Core Collection (BKCI)

Interested in publishing with us?  
Contact [book.department@intechopen.com](mailto:book.department@intechopen.com)

Numbers displayed above are based on latest data collected.  
For more information visit [www.intechopen.com](http://www.intechopen.com)



# One-Dimensional Metal Oxide Nanostructures for Chemical Sensors

*Esther Hontañón and Stella Vallejos*

## Abstract

The fabrication of chemical sensors based on one-dimensional (1D) metal oxide semiconductor (MOS) nanostructures with tailored geometries has rapidly advanced in the last two decades. Chemical sensitive 1D MOS nanostructures are usually configured as resistors whose conduction is altered by a charge-transfer process or as field-effect transistors (FET) whose properties are controlled by applying appropriate potentials to the gate. This chapter reviews the state-of-the-art research on chemical sensors based on 1D MOS nanostructures of the resistive and FET types. The chapter begins with a survey of the MOS and their 1D nanostructures with the greatest potential for use in the next generation of chemical sensors, which will be of very small size, low-power consumption, low-cost, and superior sensing performance compared to present chemical sensors on the market. There follows a description of the 1D MOS nanostructures, including composite and hybrid structures, and their synthesis techniques. And subsequently a presentation of the architectures of the current resistive and FET sensors, and the methods to integrate the 1D MOS nanostructures into them on a large scale and in a cost-effective manner. The chapter concludes with an outlook of the challenges facing the chemical sensors based on 1D MOS nanostructures if their massive use in sensor networks becomes a reality.

**Keywords:** metal oxide semiconductors, one-dimensional nanostructures, nanowires, nanofibers, heteronanostructures, chemical vapor deposition, hydrothermal synthesis, electrospinning, chemiresistors, field-effect transistors, electrohydrodynamic printing

## 1. Introduction

The chemical sensor market requires high performance on all 4S parameters: sensitivity, selectivity, speed, and stability. Moreover, the prevalence of the internet of things (IoT) and wireless sensor networks, as the technology of choice for pervasive real-time monitoring, demands miniaturized sensors with very low power and low cost [1]. Over the past few decades, metal oxides semiconductors (MOS) have been intensively used in chemical sensors for a wide variety of applications. On one hand, MOS can be produced by low-cost wet-chemical synthesis routes from earth-abundant low-cost precursors and are, in general, non-toxic. On the other hand, MOS exhibit unique electronic, chemical and physical properties that are often sensitive to changes in their environment, making them suitable for

chemical sensing [2–4]. Finally, the MOS sensors are relatively easy to be miniaturized and integrated into microfabrication processes. In this regard, the micro-electro-mechanical system (MEMS) technology has enabled the miniaturization of chemical sensors using MOS by allowing the implementation of heating and sensing elements by thin-film fabrication [5, 6]. Although, the MOS microsensors fabricated with MEMS technology are already on the market due to their balance in performance and cost, they still suffer from high power consumption and lack of selectivity. The former is connected with the high working temperatures ( $>200^{\circ}\text{C}$ ), which are necessary to activate sensing mechanisms such as redox reactions, and the latter refers to the non-specificity of MOS surfaces to gaseous analytes. Several strategies have been devised to reduce the power and control the response of the MOS sensors towards specific gases by structural and/or chemical modification of the bulk and/or the surface of the sensing material [7]. Also, a most widespread solution known as the electronic nose uses a broadly responsive array of sensors to generate complex multi-dimensional measurement data in combination with pattern recognition software to interpret the resulting signal pattern [8]. Another strategy relies on the operation of sensors in dynamic mode; this implies the active variation of control parameters such as the working temperature or bias voltage by the sensor electronics, allowing application-specific optimization of the sensor performance or the target application [9, 10]. Finally, UV light-activation has been exploited for the room-temperature operation of the MOS sensors with improved detection capabilities such as sensitivity, selectivity, or response/recovery time [11].

In this context, nanotechnology has emerged as a very promising route to overcome the current drawbacks of the MOS chemical sensors. Enormous research efforts have been devoted to designing and developing MOS nanomaterials for chemical sensing with the ultimate goal of achieving the sensitivity and selectivity levels required for real-world applications while operating the sensors at low temperature, ideally at room temperature [12]. All this, to pave the way for a new generation of chemical sensors consuming very low or zero power using nanostructured MOS layers mounted on cheap, abundant, and easy-to-process substrate materials such as polymers, paper, or fabrics. Then, the fabrication costs of the MOS sensors could be reduced by using state-of-the-art technologies to pattern the electrodes and the MOS nanostructures on top of the substrate, making it possible to produce chemical sensors on a large scale [13]. This would facilitate the introduction of chemical sensors based on MOS in growing markets such as smartphones and wearable devices.

Nanomaterials of all dimensionalities (0D, 1D, 2D, and 3D) and diversity of MOS such as  $\text{TiO}_2$ ,  $\text{ZnO}$ ,  $\text{SnO}_2$ ,  $\text{CuO}$ ,  $\text{NiO}$  and many others are being investigated for high-performance detection of gases, chemicals and biomolecules [14–20], mainly for applications in the fields of environmental monitoring, healthcare and health diagnostics [21, 22]. Nanomaterials serve as building blocks for the assembly of nanostructured layers with high surface area and porosity, leading to more sensitive and faster chemical sensors. Furthermore, novel synthesis techniques allow fine-tuning of the composition, morphology, and structure of the nanomaterials' surface, which, together with possible alterations in the electronic and chemical properties at the nanoscale, could contribute to enhancing the chemical affinity of the MOS nanostructures for specific species [23, 24]. Recently one-dimensional (1D) MOS nanostructures have gained increased attention for chemical sensing because they are more applicable to nanoelectronics and nanodevices due to their high-surface-area-to-volume ratio 1D morphology [25, 26]; this means that a significant fraction of the atoms is surface atoms that participate actively in surface reactions. In 1D nanostructures the width and thickness are confined to the nanoscale, while the length spans from the micrometric to the millimetric range,

allowing 1D nanostructures to contact the microscopic and macroscopic world for many physical measurements.

This chapter surveys the latest achievements in the design and development of 1D MOS nanostructures for chemical sensing. The focus lies on conductometric sensors, specifically resistive and field-effect-transistor-based (FET) sensors, where MOS finds the broadest application. Also, this survey is limited to the 1D nanostructures that have demonstrated the greatest potential for use in conductometric sensors, namely nanowires and nanofibers. Other 1D nanostructures such as nanorods, nanotubes, nanobelts, nanoribbons, or nanoneedles have also been investigated, but to a lesser extent. The techniques for the synthesis of nanowires and nanofibers based on MOS are presented and discussed in terms of their complexity, the potential for integrating the 1D MOS nanostructures into sensor architectures and scalability. Finally, the chapter summarizes the challenges ahead and the prospects for progress in this field.

## **2. Sensitive materials**

The heart of a chemical sensing device is the sensing element or sensor, which consists of two components: a receptor and a transducer. The receptor is the sensitive or active material that has an affinity for and interacts with a specific analyte, stimulating the transducer and causing a change in some physical or chemical property of the material that is ultimately converted into an electrical signal. The analyte may be chemical species (e.g., molecules, ions) or biological species (e.g., microorganisms, biomolecules) in the gas or liquid phase. The receptor function may rely on various principles: physical, where no chemical reaction takes place; chemical, in which a chemical reaction with the participation of the analyte gives rise to the analytical signal; and biochemical, when a biochemical process involving the analyte and a biological recognition element is the source of the analytical signal. The latter is called a biosensor, which is regarded as a subgroup within the group of chemical sensors. According to the operating principle of the transducer, chemical sensors may be classified as optical, electrochemical, electrical, gravimetric, magnetic or thermometric [27]. In electrically-transduced sensors, the signal arises from the changes in the properties of the sensitive material such as conductivity, work function, or permittivity. These changes are converted into variations in electrical parameters of the sensor such as capacitance, inductance or resistance and finally into changes in the device current or voltage. Electrically-based sensors are one of the most investigated chemical sensors due to their simplicity, portability, compatibility with standard electronics, non-line-of-sight detection, the capability of continuous monitoring and potential for wireless transmission.

### **2.1 Metal oxide semiconductors**

MOS has been used as primarily sensitive materials in conductometric chemical sensors due to their outstanding physical and chemical properties. MOS can be produced by a large number of cost-effective synthetic methods, have shown to be active to detect chemical analytes, and their energy band alignment has proved to be suitable to immobilize biomolecules (e.g., enzymes, antibodies, DNA) [2, 18]. MOS are classified according to their conductivity as n-type and p-type, in which the charge carriers are electrons and holes, respectively. N-type MOS (e.g., SnO<sub>2</sub>, ZnO, TiO<sub>2</sub>, In<sub>2</sub>O<sub>3</sub>, WO<sub>3</sub>, V<sub>2</sub>O<sub>5</sub>) are the most representative materials for sensing gases and bioanalytes. Some of them are already commercially used, as it is the case in gas sensors, due to their higher sensitivity compared to p-type MOS (e.g., NiO, CuO, Co<sub>3</sub>O<sub>4</sub>, Cr<sub>2</sub>O<sub>3</sub>, Mn<sub>3</sub>O<sub>4</sub>) or other MOS that present both n- and

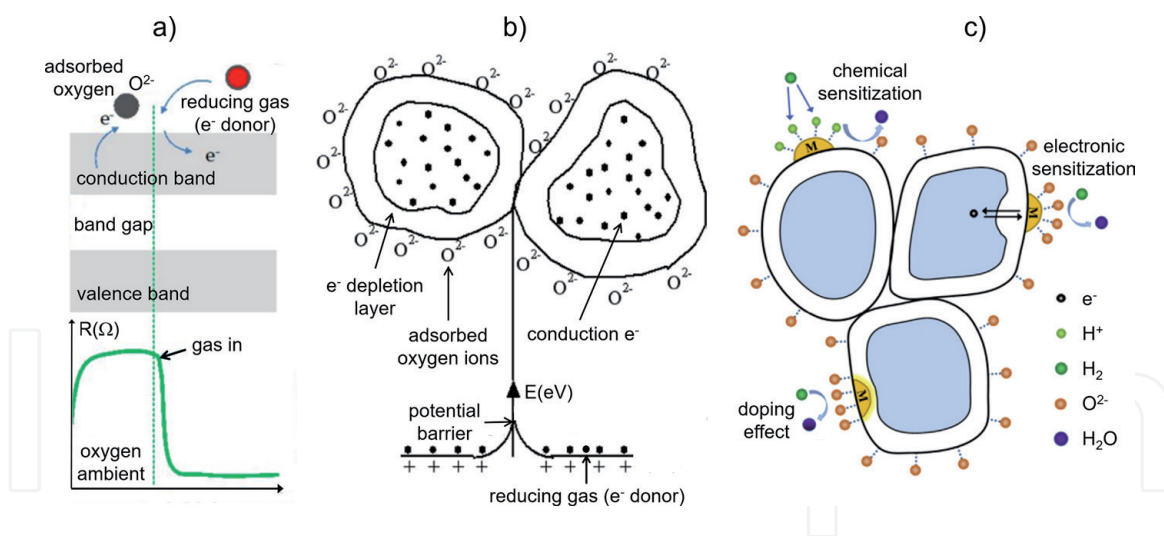


**Figure 1.**

*Schematic illustration of the sensing mechanisms in an n-type metal oxide semiconductor: (a) Interaction with ambient oxygen and with a reducing gas and variation of the sensor resistance; adapted with permission from [32], Copyright 2012 Authors, licensee IntechOpen. (b) Electron depletion layer at the grain surface and intergrain barrier potential; adapted with permission from [33], Copyright 2012 Authors. (c) Hydrogen detection mechanisms in a metal oxide semiconductor functionalized with metal nanoparticles; adapted with permission from [51], Copyright 2018 Elsevier.*

p-type behavior (e.g.,  $\text{Fe}_2\text{O}_3$ ,  $\text{HgO}_2$ ) [28, 29]. Also, n-type MOS are thermally stable and have the possibility to work at lower partial pressure, in contrast to p-type MOS which are less stable due to their tendency to exchange lattice oxygen easily with air. Another practical reason for the use of n-type MOS in conductometric sensors is related to the preferred direction for resistance change during detection of reducing gases (the vast majority of gaseous analytes), which simplifies the peripheral electronics for measurements and improves the reproducibility of the output signal. Nonetheless, p-type MOS should not be underestimated as sensitive materials, as significant improvement in sensor performance can be achieved by incorporating p-type MOS with commonly used n-type MOS [30]. As an example, p-type MOS have been used as good catalysts to promote selective oxidation of various volatile organic compounds. Moreover, the distinctive oxygen adsorption of p-type MOS may be used to design high-performance gas sensors that show low humidity dependence and rapid recovery speed [31].

**Figure 1a** and **b** illustrate the sensing mechanisms in an n-type MOS [32, 33]. The molecules of the ambient oxygen are adsorbed and then ionized by capturing electrons from the conduction band. Thus, an electron depletion layer of a given width, known as Debye length, forms at the surface of the MOS grains and a potential barrier develops at the boundaries of adjacent grains, caused by the negative surface charge due to the adsorbed oxygen ions. As a result, the density of free electrons is reduced and the electron conduction is hindered, increasing the sensor resistance. In the presence of a reducing gas (electron donor), the gas molecules react with the adsorbed oxygen ions, which are released to the ambient, while the trapped electrons return to the conduction band. Then, the density of free electrons increases and the intergrain barrier potential is reduced, resulting in a decrease in the sensor resistance. Many optimization strategies aim at modulating or triggering variations in the electron depletion region or barrier potential in a controlled manner to improve the receptor function in chemical sensors based on MOS.

## 2.2 Functionalized metal oxide semiconductors

Since the efficiency of the chemical receptor material is surface-dependent, previous research on MOS sensors proved that MOS with sizes within the Debye

length, typically of the order of 2–100 nm, are attractive in chemical sensing as they provide higher surface-area-to-volume-ratio, as compared to bulk materials. Also, it was found that nanostructures (e.g., 1D MOS) can provide specific crystal facets and electronic properties to the surface that enhance the performance of the receptor [34]. Further, the functionalization or modification of MOS nanostructures by loading, doping, surface-decoration or hybridization with second-phase constituents (e.g., noble metals, other MOS, carbon-based materials) showed other ways to enhance and extend the capabilities of the receptor [35, 36]. Similarly, in biochemical sensors, the functionalization of the surface by immobilizing biomolecules that act as biological recognition elements of specific analytes (e.g., glucose, urea, cancer cells, viruses) is mandatory to sensitize the MOS surface [2, 18, 37].

The rationale for these improvements or further sensitization is generally connected with an increase in the density of active sites (e.g., defects, oxygen vacancies) or charge carriers (doping effect). Also, it is related to the catalytic activation (chemical sensitization) and the formation of interfaces (electronic sensitization), either metal-semiconductor or semiconductor-semiconductor interfaces. The latter is known as heterojunctions as they involve two dissimilar semiconductors, whilst the combination of multiple heterojunctions together in a system is called a heterostructure. The materials chosen for these interfaces dictate the principles of sensing; for example, in gas sensing, adsorption, reaction, and electronic behavior. On one side, the intimate electrical contact at the interface between the two components equilibrates the Fermi level across the interface to the same energy, usually resulting in charge transfer and further extending the region of charge depletion/accumulation. On the other side, the mix of the two components leads to synergistic behavior. This means that each component serves a different purpose that is complementary to the other, so that the synergistic effect of the two-component system is greater than the effect of each element. The synergistic effect is possible due to three common features: geometric effects, electronic effects, and chemical effects. These are the basis for the improved sensing properties such as enhanced sensitivity and recovery speed or reduced operating temperature of the MOS heteronanostructures [38–42]. These approaches are also used to improve further the selectivity, particularly towards gas analytes. The usual combination includes wide bandgap MOS of n-type as the host material and second-phase constituents commonly chosen from noble metals (e.g., Pt, Pd, Ag, Au) [43–45] or other transition metal oxides (e.g., p-type: NiO, CuO, Cr<sub>2</sub>O<sub>3</sub>, Fe<sub>2</sub>O<sub>3</sub>, Co<sub>3</sub>O<sub>4</sub>, Mn<sub>3</sub>O<sub>4</sub>; n-type: SnO<sub>2</sub>, ZnO, In<sub>2</sub>O<sub>3</sub>, WO<sub>3</sub>, TiO<sub>2</sub>) [46, 47]. Recent combinations also make use of carbon-based materials (e.g., carbon nanotubes, graphene) [48, 49] and two-dimensional (2D) inorganic materials (e.g., transition metal dichalcogenides TMDC, transition metal carbides and nitrides MXenes, phosphorene) [50].

Generally, the modifiers or additives (i.e., metals, MOS, rGO) enhance the sensing properties of the host MOS by surface- (chemical sensitization) and/or interface- (electronic sensitization) dependent effects. As an example, **Figure 1c** illustrates the synergistic mechanisms, both chemical and electronic, enabling the detection of hydrogen by a MOS functionalized with metal nanoparticles [51]. The chemical sensitization includes spill-over (i.e., the enrichment of the MOS surface with reactive species through catalysis), whereas the electronic sensitization involves Fermi level control (i.e., changes in the chemical state of the additive with active species). To date, there is no clear evidence of whether any of these mechanisms are superior. Nevertheless, the literature indicates the need to combine both mechanisms to induce a better performance of MOS. The possibility of tuning the sensor performance via chemical and electronic sensitization depends strongly on the characteristics (size, shape, distribution, composition, oxidation states) of the MOS and additives forming the heteronanostructure and the formation of an

intimate electric contact at the interface of the components. The optimal combination of components significantly improves the selectivity and sensitivity of MOS sensors to specific gases, especially for sensors operated at room temperature.

In summary, MOS nanomaterials modified with second-phase materials and controlled interfaces are essential for sensing chemical species more efficiently. Among several nanoscale materials, 1D structures have been shown to be most relevant to chemical sensing. They are projected as potential structures for molecular-level sensing, particularly when integrated as single elements. Below are discussed the most common synthetic methods to achieve 1D MOS nanostructures and their integration with appropriate transducers for their application as chemical sensors.

### 3. Synthesis of 1D metal oxide nanostructures

Among a host of 1D nanostructures, nanowires and nanofibers bring the greatest potential for use in the next generation of chemical sensors based on MOS [52–60]. Both nanomaterials have a high specific surface area and a large surface-area-to-volume ratio. However, their aspect ratio, crystallinity and surface properties may differ markedly because of the different synthesis techniques and conditions used, which in turn result in different chemical sensing performances. The techniques for the synthesis of 1D MOS structures can be classified in two general approaches: top-down and bottom-up technologies. Top-down technologies are subtractive technologies that rely on microfabrication methods, mainly lithography and etching processes, to reduce the lateral dimensions of a MOS film to nanometer size. Usually, the 1D nanostructures produced by this approach are amorphous or polycrystalline structures. Top-down technologies are well developed in the semiconductor industry, but need expensive equipment limiting their broad application in the academic sector. Bottom-up technologies, in contrast, are additive technologies that consist of the assembly of molecular building blocks that lead to the formation of nanostructures. Bottom-up technologies are generally enabled by vapor- or solution-based techniques and are considered cost-effective solutions for large-scale production of 1D nanostructures [24]. The nanomaterials produced by this approach may have monocrystalline or polycrystalline characteristics depending upon the specific processing steps of the vapor- or solution-based techniques employed.

Different routes are commonly used to synthesize 1D MOS nanostructures [61–63]. Whist chemical vapor deposition (CVD) is one of the most representative vapor-phase methods for forming 1D nanostructures; hydrothermal synthesis and electrospinning-assisted synthesis are the most representative amongst the liquid-phase methods. However, CVD and hydrothermal synthesis share common mechanisms for 1D structure formation based on nucleation and growth processes, whereas 1D structures formed by electrospinning rely on the generation of guiding polymer-based fibers using an electrostatic field to shape the 1D structure. The following sub-sections discuss separately the synthesis of 1D MOS nanostructures based on nucleation and growth processes and those mediated by electrospinning, herein called nanowires and nanofibers, respectively. A sub-section dedicated to the functionalization of these 1D nanostructures with second-phase materials is also included in this section.

#### 3.1 Synthesis of nanowires based on nucleation and growth processes

The group of synthetic methods employed to form chemical-sensitive 1D structures usually involves CVD and hydrothermal processes. Generally, CVD refers to

methods based on chemical reactions of gaseous reactants in an activated environment. In CVD synthesis, chemical precursors in the vapor phase are delivered to a reactor, where external energy (heat, light, or plasma) is added to the system to initiate the deposition reactions. These reactions can be homogeneous or heterogeneous; the first occurs in the gas phase whilst the second occurs between gas-phase species and a solid substrate (usually involving an initial gas phase reaction with the formation of reactive intermediate species). Homogeneous reactions form typically non-adherent powders and by-products whereas heterogeneous reactions lead to nucleation and growth processes on solid substrate surfaces that result in the formation of a solid material [64]. Tuning the reaction conditions by adjusting pressures, precursors, and type of activation, amongst other CVD-type related parameters, can promote the formation of either planar films or 1D structures such as nanowires. In contrast, hydrothermal synthesis refers to chemical reaction methods run in a sealed and heated aqueous solution at appropriate temperatures (100–1000 °C) and pressures (1–100 MPa); the name solvothermal is commonly used when organic solvents are involved in the solution. In hydrothermal/solvothermal synthesis, the properties of the synthesized structures are controlled by adjusting parameters such as the solution pH, the chemical species concentration, and the oxidation-reduction potential, apart from the temperature and pressure. The nucleation of the structures can also be adjusted by adding inorganic additives. Thus, hydrothermal/solvothermal synthesis can generate large good quality crystals while keeping control over the material composition [65]. Both CVD and hydrothermal/solvothermal methods have been suitable to deliver MOS nanoparticles and nanostructures including nanowires of ZnO [66–68], SnO<sub>2</sub> [68, 69], or WO<sub>3</sub> [70, 71], to cite a few examples. The formation of nanowires by these methods generally responds to two mechanisms: one assisted by adding catalyst seeds and the other without catalysts.

### 3.1.1 Mechanisms involving catalyst

This growth mechanism is characterized by the use of molten metal catalysts over the substrate that can rapidly adsorb a fluid (in gaseous, liquid, or supercritical phase) containing the MOS precursor to supersaturation levels. According to the type of fluid, this mechanism is known as vapor-liquid-solid (VLS), solution-liquid-solid (SLS) or supercritical-fluid-liquid-solid (SFLS) [24, 72, 73]. The adsorption of the fluid can be molecular or dissociative followed by adatoms diffusion on the catalyst, the substrate, or the nanowire sidewalls. Diffusion across the substrate and the sidewalls needs to be rapid to avoid nucleation events. In this regard, the nanowires can grow from the top or from the bottom of the catalyst as single nanowires, as depicted in **Figure 2a–c**, respectively [74]. In many cases, there is a one-to-one correspondence between the catalyst particle size and the nanowire, although this is not a rule. Multiple nanowires can also grow, without

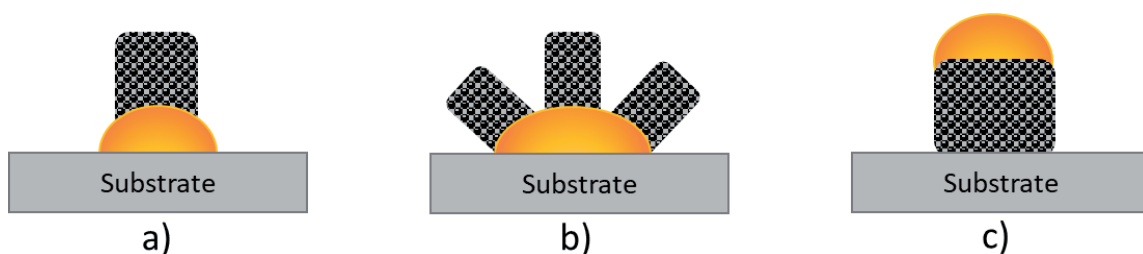


**Figure 2.** Catalytic growth of nanowires from (a and b) the top and (c) the bottom of the catalyst particle. Nanowires in (a) and (c) may have a one-to-one correspondence with the catalyst particle size, whereas wires in (b) do not have direct correspondence with the catalyst particle size; reprinted from.

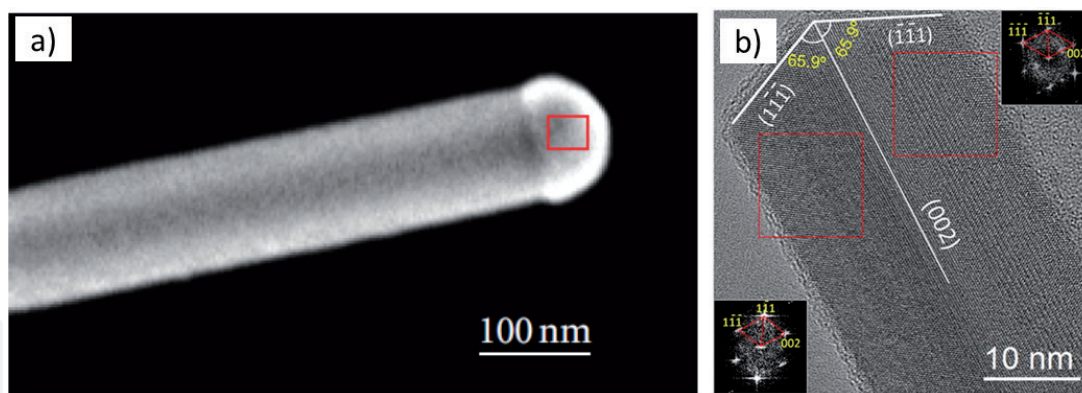


**Figure 3.**

(a) High-resolution SEM image of a ZnO nanowire grown by VLS mechanism using binary alloy of Cu/Au as a catalyst; reprinted with permission from [75], Copyright 2012 Authors. (b) HRTEM image of CuO nanowires grown by non-catalytic mechanism assisted by twin boundary defects (the insets show fast Fourier transform images from the areas of the crystals indicated by red squares); reprinted with permission from [78], Copyright 2014 American Chemical Society.

direct correspondence with the catalyst size, but with other structural factors such as the curvature and lattice matching at the catalyst-nanowire interface. VLS- and SFLS-related methods have a wide selection of catalysts (Au is the most common) and deliver high-quality nanowires with wide synthetic tunability. However, they usually require high temperature ( $>400\text{ }^{\circ}\text{C}$ ) and/or high pressure, and specialized equipment. SLS-related methods, in contrast, have the advantage of requiring low temperature ( $200\text{--}350\text{ }^{\circ}\text{C}$ ), although this fact restricts to a certain degree the choice of catalyst to low melting point catalyst such as Ga, In, or Sn. These mechanisms have brought up discussions of whether the catalyst particles reach a liquid-phase or stay in the solid phase. Nevertheless, and since any of these possible ways is ruled out, currently one can also find literature reports that state the growth of nanowires by vapor-solid-solid (VSS), solution-solid-solid (SSS), or supercritical-fluid-solid-solid (DFSS) mechanisms, with the results suggesting that the dynamics of nanowire growth is not affected by the phase of the catalyst particle [72]. An example of ZnO nanowires grown by VLS using binary alloy of Cu/Au as the catalyst is displayed in **Figure 3a**) [75]. Cu/Au catalysts have better adhesion properties than pure Au catalysts providing advantages to pattern vertically aligned nanowires as demonstrated for ZnO nanowires.

Catalytic growth of nanowires brings a fine control over the wire geometry, specially diameters and lengths. However, the nanowires yielded by catalyst-based routes incorporate catalyst atoms (impurities) into their structure, influencing the nanowires' physical and chemical properties and possible intended applications. Therefore, non-catalytic alternative routes (without using catalyst particles) are also being used and explored to grow nanowires. The next sub-section deals with this type of mechanism.

### 3.1.2 Mechanisms without catalysts

Also known as the catalyst-free growth mechanism. It is usually represented by the vapor-solid (VS) growth mechanism, although it also includes other growth processes, such as those assisted by defects or droplets. In the vapor-solid (VS) growth, mass transport is achieved preferably from the vapor phase. The nanowire crystallization originates from the direct vapor condensation, without needing the assistance of defects. In this process, the initially condensed molecules form seed crystals that serve as nucleation sites. Once an atomic layer is nucleated, the subsequent atomic layers grow at a faster rate than the wire edge, whose edge is

consumed by mass transport to the newly formed layer [63, 76]. Previous, *in-situ* TEM observations of catalyst-free VS grown tungsten oxide nanowires showed that the wires' edges grow approximately 20 times slower than the newly formed atomic layers [77]. Non-catalytic growth of nanowires assisted by defects, in contrast, relies on line defects that act as nucleation centers. In this type of growth, mass transport can be provided from a vapor or by adatoms diffusion along with the growing structure. Previous reports connect the final 1D morphological structure with the defect types. For instance, defects such as screw dislocations showed to lead to nanowires with cylindrical shape [76], whereas planar defects (twin boundaries) have proved to serve as points for preferential nucleation (reducing the nucleation energy barrier) on the nanowire tip and lead to prism-like 1D morphologies [78], as shown in **Figure 3b**.

The group of non-catalyst mechanisms can also involve growth processes assisted by liquid native droplets (form by the native metal of a MOS, e.g., Cu for CuO, or Zn for ZnO). Due to the consumption or crystallization of the metal droplet during reactions and nanowire growth, these metal droplets are not considered as catalysts, despite the nanowire growth process following similar principles to those of catalyst growth via the VLS mechanism. Hence, the nanowires yielded utilizing native metal droplets do not display the droplets at the top/bottom of the wire structure or introduce impurities as in VLS [76]. Previous experiments corroborated this growth mechanism by *in-situ* TEM analysis of Al<sub>2</sub>O<sub>3</sub> nanowires grown from Al liquid particles. The studies revealed a layer-by-layer growth at the Al liquid droplet and Al<sub>2</sub>O<sub>3</sub> nanowire interface, promoted by the surrounding oxygen and Al<sub>2</sub>O gases, following the so-called oscillatory mass transport, which is also characteristic in the growth of the nanowires by VLS and VS [79].

### 3.2 Polymer-assisted synthesis of nanofibers

Metal oxide nanofibers can be synthesized by chemical bottom-up routes like the ones described in the previous sub-section, as well as by top-down routes either mechanical or spinning methods [80–82]. Among the latter, electrospinning is the most widely used method for the production of metal oxide nanofibers, mainly due to its high simplicity and ease of use, low-cost setup, ability to mass-production of continuous fibers, and flexibility in controlling the diameter, morphology, structure, and alignment of the fibers [82–84]. The typical setup for electrospinning is depicted in **Figure 4a**) [85]. This is rather simple and operates at ambient conditions, although the mechanism of electrospinning is complex [86, 87]. An

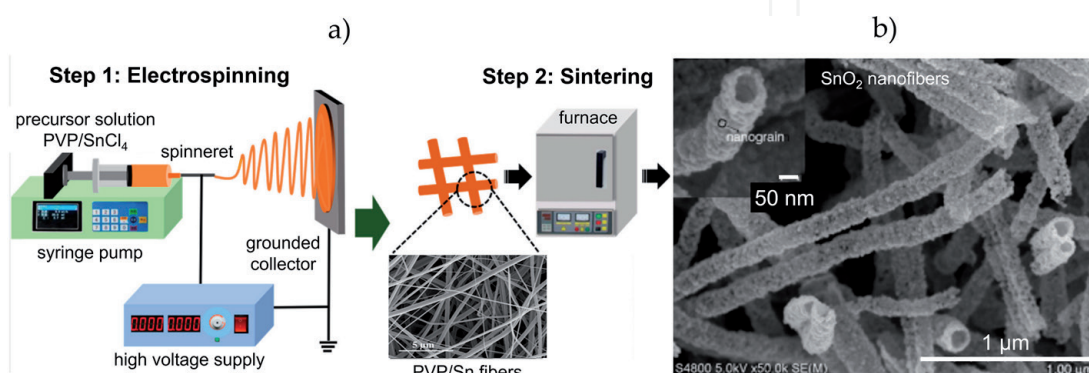


**Figure 4.** (a) Schematic illustration of the synthesis of SnO<sub>2</sub> nanofibers by (step 1) electrospinning of the precursor solution followed by (step 2) high-temperature sintering of the as-spun fibers; adapted with permission from [85], Copyright 2018 Authors, licensee MDPI. (b) SEM micrograph of the hollow SnO<sub>2</sub> nanofibers resulting from (a); reprinted with permission from [97], Copyright 2013 eXpress Polymer Letters.

electrospinning system consists of three major components: a high voltage supply, a spinneret (e.g., glass capillary tube, metallic needle, pipette tip) and a grounded collector. The high voltage source injects the charge of a given polarity into a polymer solution, which is fed (e.g., syringe pump) at a constant rate to the spinneret. An electric field is thus established between the spinneret and the collector and when it reaches a critical value, the liquid reaching the spinneret tip forms a cone (Taylor cone) that emits a liquid jet through its apex. This charged liquid jet is stable only at the tip of the cone and undergoes an unstable and rapid stretching and whipping process downstream of the spinneret, which leads to the formation of a long and thin thread. As the liquid jet is continuously elongated and the solvent is evaporated, its diameter can be reduced from hundreds of micrometers down to the sub-micrometer scale. The electrospun polymer fibers are deposited randomly on the plate due to the attraction of the collector placed in front of the spinneret.

The diameter, morphology, and structure of the electrospun fibers are key factors that need to be controlled for practical applications [88, 89]. They depend on a multitude of parameters related to the solution, setup and electrospinning process [90–94]. Target fibers can be obtained by properly choosing the polymer and the solvent and their concentration in the solution, thereby adjusting the electrospinning-relevant solution properties such as viscosity, surface tension, and electrical conductivity. The setup orientation (e.g., vertical, horizontal), spinneret type (e.g., needleless, single-needle, coaxial-needle) and nozzle diameter, solution feed rate, applied voltage, and spinneret-to-collector distance tremendously influence the fiber features. These features are also affected by the evaporation conditions such as ambient temperature and humidity.

Nanofibers of the MOS used for chemical sensing can be produced by electrospinning of a solution containing a polymer (e.g., polyvinylpyrrolidone PVP, polyvinylalcohol PVA, polyvinylacetate PVAc, polyethylene oxide PEO) and an inorganic precursor (e.g., acetates, nitrates, chlorides) in a solvent (e.g., deionized water DIW, ethanol EtOH, isopropyl alcohol IPA, dimethyl formamide DMF) followed by a sintering step, also known as annealing or calcination, at high temperature [84, 95, 96]. After obtaining the electrospun polymer/metal composite fibers, the polymer is eliminated by the sintering process. The evaporation of residual solvent and water from the fibers occurs in the first place, at low temperature. As the temperature rises, the polymer decomposes gradually and fiber shrinkage takes place. Simultaneously the inorganic precursor undergoes a complex transformation including outwards radial diffusion, nucleation, condensation, crystallization and oxidation processes to finally form metal oxide nanograins aligned along the preceding as-spun fibers [84]. A simplified schematic of the process is shown in **Figure 4a**) [85], while **Figure 4b**) displays the SnO<sub>2</sub> nanofibers obtained by sintering the as-spun fibers [97]. The nanofibers have diameters of less than 100 nm that are rather uniform along the entire length of the nanofibers, which are in the order of hundreds of micrometers. They are hollow nanofibers and have an ultra-thin porous granular wall consisting of SnO<sub>2</sub> nanograins.

Sintering parameters such as the heating rate, sintering temperature and time, cooling rate, and atmosphere largely influence the diameter, structural morphology, crystallinity and grain size of the MOS nanofibers [93], which in turn determine their sensing performance [98–100]. Hollow nanofibers have about twice the active surface area of solid nanofibers of the same diameter, which increases the sensor response, as gases can interact with both the outer and inner surface of the nanofibers [101]. While MOS nanowires are single-crystalline with no noticeable grains, electrospun MOS nanofibers are composed of polycrystalline grains. Higher sintering temperatures or longer sintering times result in better crystallinity, which in turn leads to higher sensor response. Also, the grain size increases with the increasing

sintering temperature and time, but the sensor response decreases with the increasing grain size due to the lower surface area. Hence, it is necessary to optimize the size and crystallinity of the grains in the MOS nanofibers simultaneously to attain superior sensing behavior [102–107]. The diameter and wall thickness of the hollow MOS nanofibers increase with the increasing concentration of polymer and inorganic precursors in the solution, respectively [108]. Reducing both the diameter and wall thickness also improves the sensing properties of the electrospun MOS nanofibers [98]. A decrease in the diameter of the nanofiber contributes to decreasing both the grain size and the time of gas diffusion into the nanofiber, resulting in enhanced sensor response and reduced response time. Nevertheless, there is a limit in the process of enhancing sensor performance by decreasing the grain size, since an excessive decrease of grain size (<10 nm) leads to a loss of structural stability and, as a consequence, to changes in both surface and catalytic properties of the material. Moreover, the porosity of the wall determines the accessibility of the gases to the inner surface of the hollow fibers, and several strategies have been adopted to increase the porosity of the electrospun MOS nanofibers. One strategy is to remove the polymer from the as-spun polymer/metal fibers by exposing the fibers to RF oxygen plasma before sintering [109, 110], as can be seen in **Figure 5**. This technique allows tuning the porous structure of the hollow MOS nanofibers by controlling the etching power and time. Finally, in a recent work 1D hierarchical structures of ZnO have been prepared by growing ZnO nanowires over electrospun polyacrylonitrile (PAN) fibers loaded with Au nanoparticles, as seeds for catalytic VLS growth [111]. **Figure 6** shows the resulting ZnO cactus-like structures, whose surface area is far larger than that of electrospun ZnO nanofibers of the same diameter.

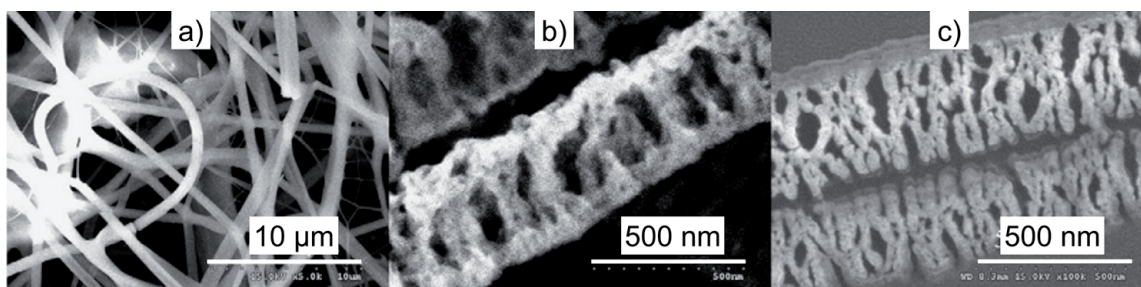


**Figure 5.** SEM micrographs of electrospun PVA/Sn fibers (a) without post-treatment and (b) after exposure to RF oxygen plasma, (c) highly porous hollow SnO<sub>2</sub> nanofibers obtained by sintering of the PVA/Sn fibers in (b). Reprinted with permission from [110], Copyright 2009 Elsevier.

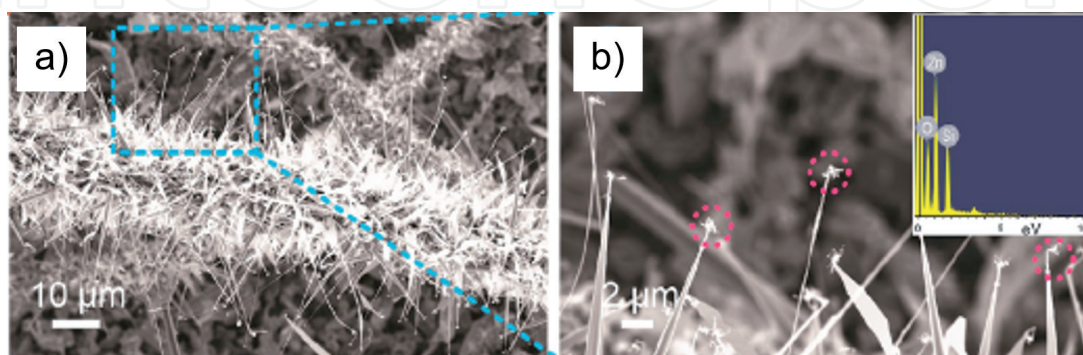


**Figure 6.** (a) SEM micrograph of a ZnO nano-cactus like structure obtained by VLS growth of ZnO nanowires over electrospun fibers of polyacrylonitrile (PAN) loaded with Au nanoparticles. (b) Higher magnification SEM micrograph of the dashed area in (a), showing Au nanoparticles at the tip of ZnO nanowires (dotted circles) and EDX spectrum of the ZnO structure (inset). Reprinted with permission from [111], Copyright 2021 Elsevier.

### 3.3 Functionalization of 1D metal oxide nanostructures

Functionalization or modification with second-phase constituents (modifiers or additives) can strongly change the physical and chemical properties of the 1D MOS nanostructures. Tailoring the properties (e.g., shape, size, load, dispersion) of the additives is a very challenging task because not all methods allow for the control of their properties and homogeneous dispersion over the 1D MOS nanostructures. The functionalization or modification of 1D MOS nanostructures with second-phase materials may be of the decorative-type, only at surface level, when incorporating low amounts of the additives at the surface. It can also involve single mixtures, when mixing 1D nanostructures and the additives randomly, or doping, when additive atoms incorporate in the intrinsic material structure [25, 112]. Generally, the methods to functionalize or modify 1D MOS nanostructures fall into two categories: one-step processes in which the additive materials are incorporated simultaneously during the 1D nanostructure formation or multiple-step processes in which the additives are incorporated over the pre-synthesized 1D MOS nanostructures [113]. In both cases, the incorporation may involve a precursor for the targeted additive or pre-formed particles, as shown in **Figure 7**. Routes 1 and 2 (representing one-step processes) may be enabled by sol-gel, hydrothermal synthesis, CVD, and electrospinning. Routes 3 and 4 (representing multiple-step processes) rely on techniques, such as dip- or spin-coating, to introduce pre-formed additives or a broad type of techniques that can incorporate the additive from a precursor or as ions. For instance, high energy ion implantation, immersion in solutions containing the additive precursor followed by a photocatalytic reduction or heat treatment, sputtering, hydrothermal synthesis, CVD including atomic layer deposition (ALD), amongst others.

1D heteronanostructures have gained great attention due to their hybrid properties, which may induce synergies between the host material (MOS) and the guest material (modifier or additive), resulting in improved and/or new attributes for the chemical detection [114–116]. In the first place, p-type MOS of transition metals (e.g., CuO, NiO, Fe<sub>2</sub>O<sub>3</sub>) and noble metals (e.g., PdO, Ag<sub>2</sub>O) have been applied to develop ultrasensitive chemical sensors by tuning the electrical properties of the n-type MOS by forming n-p heterojunctions. Also, n-n heterojunctions may lead to enhanced sensing performance of the nanostructures composed of two n-type MOS with different work functions (e.g., SnO<sub>2</sub>-ZnO, WO<sub>3</sub>-SnO<sub>2</sub>, TiO<sub>2</sub>-SnO<sub>2</sub>, SnO<sub>2</sub>-In<sub>2</sub>O<sub>3</sub>), as compared to single-phase MOS nanostructures. In addition, the combination of MOS and graphene may significantly improve the performance of MOS gas sensors

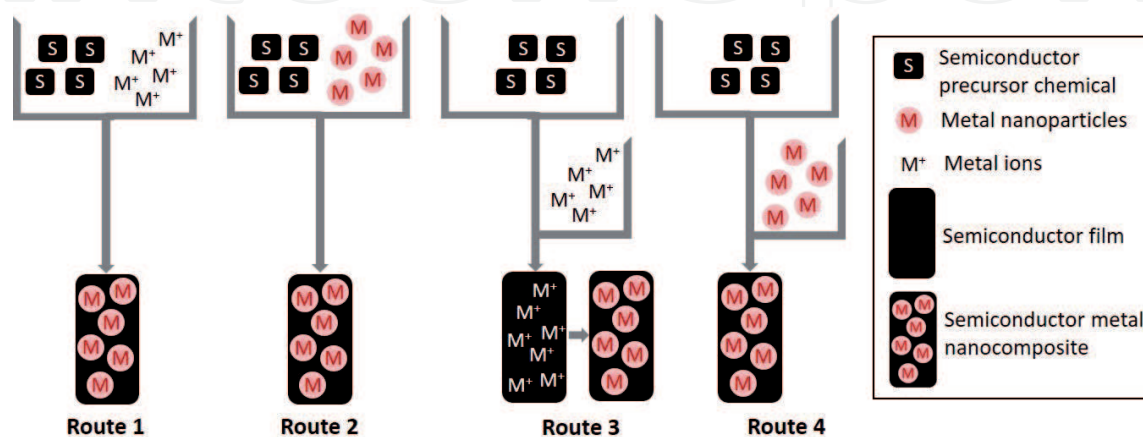


**Figure 7.**

*Routes to the functionalization or modification of 1D MOS nanostructures with second-phase materials (modifiers or additives); adapted with permission from [113], Copyright 2006 American Chemical Society.*

at room temperature [48, 117]. Graphene is a family of two-dimensional (2D) nano-materials (e.g., pristine graphene PG, graphene oxide GO, reduced graphene oxide rGO, graphene quantum dots GQD, graphene nanoplatelets GnP) that are obtained from natural graphite or synthesized chemically from organic compounds, and have different morphology, physical, chemical, and electronic properties. Among them, rGO is the best choice for gas sensing applications because it has oxygen functional groups, defects and vacancies on its surface, which favor the adsorption of gases. Moreover, rGO behaves as a p-type semiconductor and is stable at high temperature [118, 119]. When added to 1D MOS nanostructures, rGO nanosheets can increase the overall sensing surface and adsorption sites, and form n-p or p-p type heterojunctions with the MOS grains, thereby modulating the resistance of the MOS gas sensors. Also, noble metals (e.g., Au, Ag, Pt, Pd) and transition metals (e.g., Ni, Cu, Co) act as effective modifiers or additives, particularly due to their catalytic properties.

The functionalization or modification of 1D MOS nanostructures based on nucleation and growth processes usually rely on two-step processes, in which the second-phase material is incorporated in a subsequent step after the synthesis of the 1D nanostructure; routes 3 and 4 in **Figure 7**. Hence, the methods for the functionalization step are varied. They may include, for instance, sputtering as in recent reports that showed the incorporation of DC pulsed sputtered Au nanoparticles over the surface of hydrothermally synthesized ZnO nanowires, as displayed in **Figure 8a**) [120]. In this method, the size and density of the Au nanoparticles decrease as the sputtering pressure increases (e.g., from 5 to 20 mTorr) due to the dependency of the mean free path and rate of gas phase collisions on the process pressure. The routes to functionalize 1D nanostructures in a second-step process also involve a broad variety of CVD methods. Among them, for instance, aerosol-assisted (AA) CVD has demonstrated to be useful to incorporate both metals and MOS nanoparticles over 1D nanostructures. This method allowed for the incorporation of dispersed nanoparticles based on n-type or p-type MOS from metals such as Pd [121], Ni, Co, or Ir [122]. It also allowed for the formation of core-shell 1D nanostructures based on  $\text{WO}_3$  nanowires covered by a  $\text{Ce}_2\text{O}_3$  thin film [123]. Similarly, flame-assisted CVD has shown to functionalize 1D nanostructures including  $\text{SnO}_2$  nanowires with Au and Pd nanoparticles [124]. This method has also been used to modify the surface of  $\text{SnO}_2$  nanowires with an amorphous carbon layer [125]. Other methods for functionalization in a second-step may also combine the merits of several techniques, including sol-gel, dip-coating, and flame spray pyrolysis, as is the case of the sol-flame method. This method incorporates the second phase

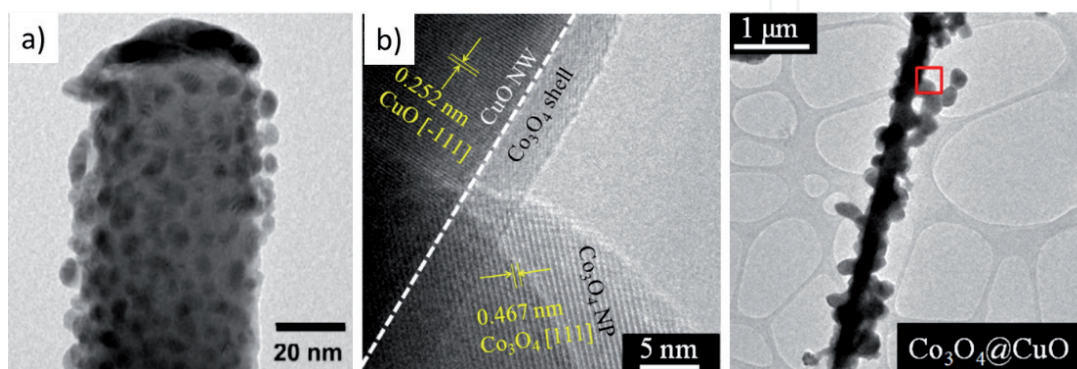


**Figure 8.** (a) TEM micrograph of a ZnO nanowire functionalized with sputtered Au nanoparticles; reprinted with permission from [120], Copyright 2021 Elsevier. (b) Functionalization of CuO nanowires by sol-flame: HRTEM (left) and TEM (right) micrographs of a CuO nanowire functionalized with  $\text{Co}_3\text{O}_4$  nanoparticles; reprinted with permission from [126], Copyright 2013 American Chemical Society.

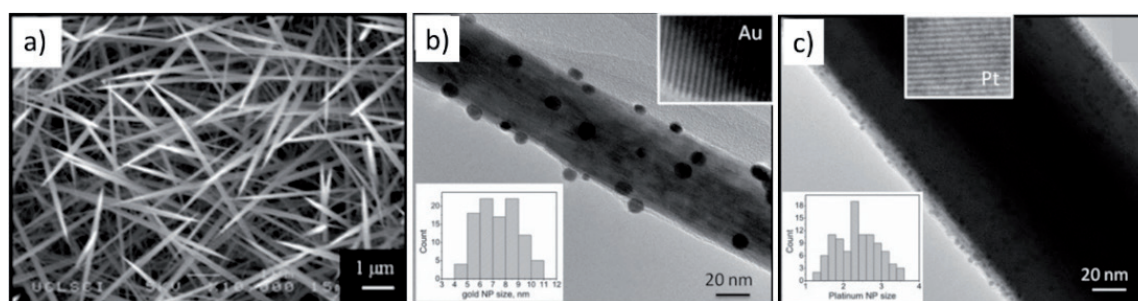


**Figure 9.** (a) SEM micrograph of  $\text{WO}_3$  nanowires functionalized with noble metal nanoparticles (Au, Pt) in a single-step process by AACVD. HRTEM micrographs of  $\text{WO}_3$  nanowires functionalized with nanoparticles of (b) Au and (c) Pt, with insets showing the size distribution and lattice fringes of the nanoparticles; reprinted from [128].

material by dip-coating the nanowires with a sol-gel precursor solution and annealing them over a flame for a few seconds. During the flame treatment, the metal salt precursor decomposes chemically to the final metal or MOS and nucleates locally over the nanowire. An example of this process used to functionalize  $\text{CuO}$  nanowires with  $\text{Co}_3\text{O}_4$  is displayed in **Figure 8b**) [126].

The functionalization or modification of 1D MOS nanostructures based on nucleation and growth processes can also be achieved by one-step processes. However, their use is less common, despite the advantage of reducing processing steps. Examples of 1D nanostructures functionalized by a one-step process include those achieved by the AACVD of two metal precursors from one-pot simultaneously [127]. In this method, the precursor leading the formation of nanowires is in a higher concentration than the precursor for the modifier. **Figure 9** displays examples of the  $\text{WO}_3$  nanowires functionalized with Au and Pt nanoparticles obtained by this method [128]. The functionalization of nanowires with MOS from metals such as Fe [129] and Cu [31] was also achieved by this method.

There is much less published work on the functionalization or modification of electrospun MOS nanofibers for application in chemical sensors than on nanowires. Most works chose to incorporate the additives or their precursors into the solution containing the polymer and the inorganic precursor of the MOS (i.e., routes 1 and 2 in **Figure 7**). Thus, for example, composite nanofibers are prepared by dissolving inorganic precursors of the involved MOS in suitable solvents and mixing the solutions with the polymer solution, usually by magnetic stirring. Then, the inorganic precursors are distributed uniformly in the polymer by electrospinning and the metals are oxidized upon sintering of the electrospun polymer/metal fibers. Intimate contact between the MOS nanocrystals is achieved in the composite nanofibers [130–133]. Another method uses the coaxial-electrospinning configuration [84, 134], for which polymer solutions are prepared with each of the inorganic precursors separately. The solution with the precursor of the main metal oxide leaves the spinneret through a central circular nozzle, while the solution with the precursor of the second metal oxide exits the spinneret through an annular nozzle that surrounds and is concentric to the circular nozzle, as depicted in **Figure 10a**) [135]. After sintering of the electrospun fibers, composite nanofibers with a core-shell structure are obtained, in which the two metal oxides occupy distinct zones with a well-defined interface [136–138], as can be seen in **Figure 10b**).

The same strategy has been adopted for the functionalization of electrospun MOS nanofibers with additives such as graphene (rGO) and metals. In this case, the rGO flakes and metal nanoparticles are dispersed or their precursors are dissolved in a liquid (e.g., DIW, EtOH, IPA), usually by ultrasonic agitation. The colloidal dispersions or solutions so obtained are added to the solution with the polymer and the

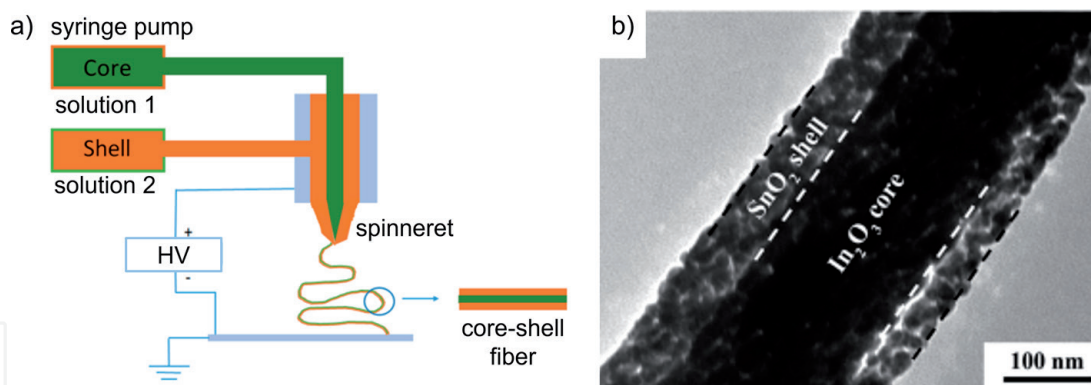


**Figure 10.** (a) Layout of a typical spinneret used for coaxial electrospinning; adapted with permission from [135], Copyright 2019 Authors, licensee MDPI. (b) TEM micrograph of an  $\text{In}_2\text{O}_3$ - $\text{SnO}_2$  core-shell nanofiber obtained by sintering of coaxially electrospun PVP/ $\text{In}$ -PVP/ $\text{Sn}$  fibers; reprinted with permission from [138], Copyright 2016 American Chemical Society.

inorganic precursor of the host MOS and, then, magnetically stirred until a homogeneous electrospinnable solution is achieved. As an example, **Figure 11** shows TEM images of an electrospun nanofiber of  $\text{SnO}_2$  loaded with rGO [139]. Double-shell hollow nanofibers are usually obtained, with the rGO nanosheets on top of the MOS nanograins [139–143]. Generally, it has been found that the rGO-loaded MOS nanofibers are more sensitive to specific gases and that the optimal operating temperature (i.e., the temperature at which the sensor response reaches a maximum) is lower than that of the pure MOS nanofibers. This improved sensing behavior is attributed to the formation of local n-p or p-p (MOS-rGO) heterojunctions.

Some authors have attempted to further improve the gas sensing capabilities of electrospun single-phase MOS nanofibers [144], MOS composite nanofibers [145, 146], and rGO-loaded MOS nanofibers [147] by functionalization of the nanofibers with metal nanoparticles. For this purpose, they chose also the routes 1 and 2 in **Figure 7**, leading to the dispersion of the metal nanoparticles, formed *in-situ* or pre-formed, in the solution with the polymer, inorganic precursors, and eventually rGO. Sensors based on hybrid nanofibers composed of  $\text{ZnO}$ , rGO and nanoparticles of Au or Pd prepared by electrospinning showed enhanced sensitivity towards reducing gases and volatile organic compounds, for the pure and rGO-loaded  $\text{ZnO}$  nanofibers [147].

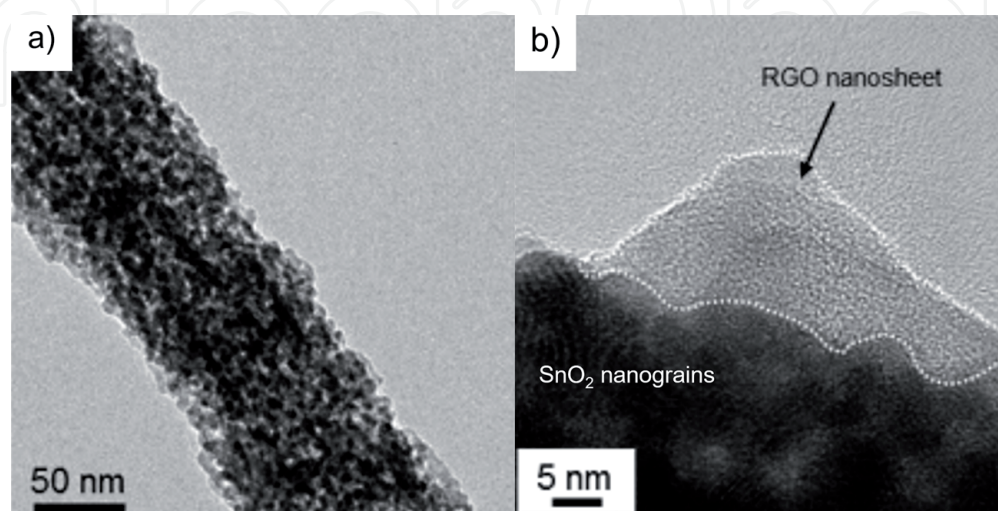


**Figure 11.** (a) Low-magnification and (b) high-magnification TEM micrographs of an rGO-loaded  $\text{SnO}_2$  nanofiber obtained by sintering of an electrospun PVA/ $\text{Sn}$ /rGO fiber; reprinted with permission from [139], Copyright 2015 American Chemical Society.

It was proven therefore the synergistic combination of the catalytic effects of the noble metal nanoparticles and the hybrid sensing mechanism, which combines the effects of radial resistance modulation, intergrain (ZnO/ZnO) modulation and local n-p (ZnO-rGO) heterojunctions. Moreover, it has been observed that there is an optimal value of the load of rGO (<1 wt%) and metal nanoparticles (1–4 wt%) in the nanofibers, above which the gas sensing performance of the hybrid nanofibers does not show further improvement or starts degrading. This result is attributed to the agglomeration of rGO nanosheets and metal nanoparticles in the polymer, resulting in the formation of agglomerates on the surface of the nanofibers and hence in an increased density of p-p (rGO-rGO) heterojunctions and metal-metal contacts, in detriment of n-p or p-p (MOS-rGO) heterojunctions and metal-MOS contacts. The electrospinning of polymer solutions containing nanomaterials is very challenging as to achieve an even distribution of the nanomaterials in the polymer fibers, since the large specific energy of the solution promotes the agglomeration of the nanomaterials [148, 149]. To overcome this problem, the nanomaterials can be loaded onto the surface of the fibers either after electrospinning or after sintering the as-spun fibers, i.e., routes 3 and 4 in **Figure 7**. This approach however adds complexity and costs as it introduces an additional process step (e.g., sputtering, ALD) for which dedicated equipment is required [150, 151].

#### 4. Integration of 1D metal oxide nanostructures into chemical sensors

The chemical sensing capabilities of the MOS have been exploited primarily in electrically-transduced sensors of the resistive and field-effect transistor (FET) types [55]. Chemiresistive sensors or chemiresistors and FET sensors are the most investigated and exploited sensing configurations owing to their simplicity, ease of fabrication and operation, and feasibility of miniaturization. The most widely used architectures of chemiresistors and FET sensors are presented in this section. There follows a discussion on the methods and techniques that allow 1D MOS nanostructures to be integrated as sensitive material into such architectures, paying attention to aspects such as sensor reproducibility and potential for scaling up sensor fabrication.

##### 4.1 Sensor architectures

Chemiresistive sensors are bipolar devices addressed to measure the electrical resistance of a semiconductor (e.g., 1D MOS nanostructure) as the sensing material bridging two electrodes or interdigitated electrodes (IDE) supported by an insulating substrate. Typically, FET sensors consist of a semiconductor (e.g., 1D MOS nanostructure) as the conducting channel connected by the source and drain electrodes. This semiconductor is placed on the top of an insulated gate electrode so that its conductance can be regulated by varying the bias voltage of the gate electrode. This classical architecture for electronic metal-oxide field-effect transistors (MOSFET) is usually similar for FET sensors addressed to gas-phase analytes. In contrast, the architecture of FET sensors for liquid phase analytes differs from the traditional MOSFET, since the gate electrode (or reference electrode) is immersed into the liquid analyte with the conducting channel being sensitive to the ions of the analyte. Therefore, this architecture is known as an ion-sensitive field-effect transistor (ISFET) [37]. **Figure 12** displays a schematic illustration of the two types of sensor architectures (resistive and FET) targeted in this section.

Nowadays, the fabrication of these transducer platforms exploits micro/nano-fabrication technologies, usually based on silicon as substrate and

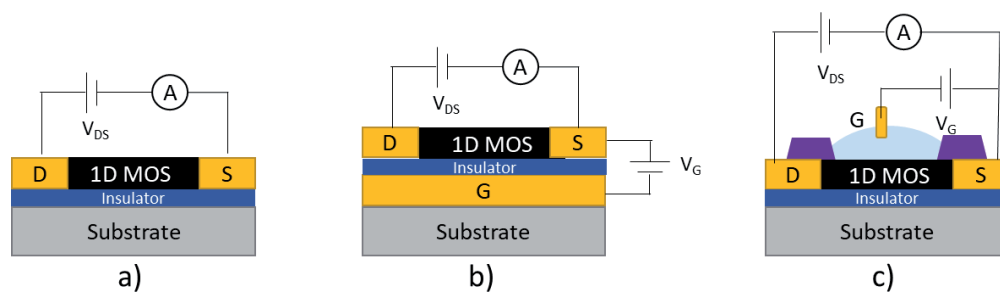


**Figure 12.** Schematic illustration of a resistive (a) and FET transducing platform for gas (b) and liquid (c) phase analytes. NW: nanowires, D: drain electrode, S: source electrode, and G: gate electrode.

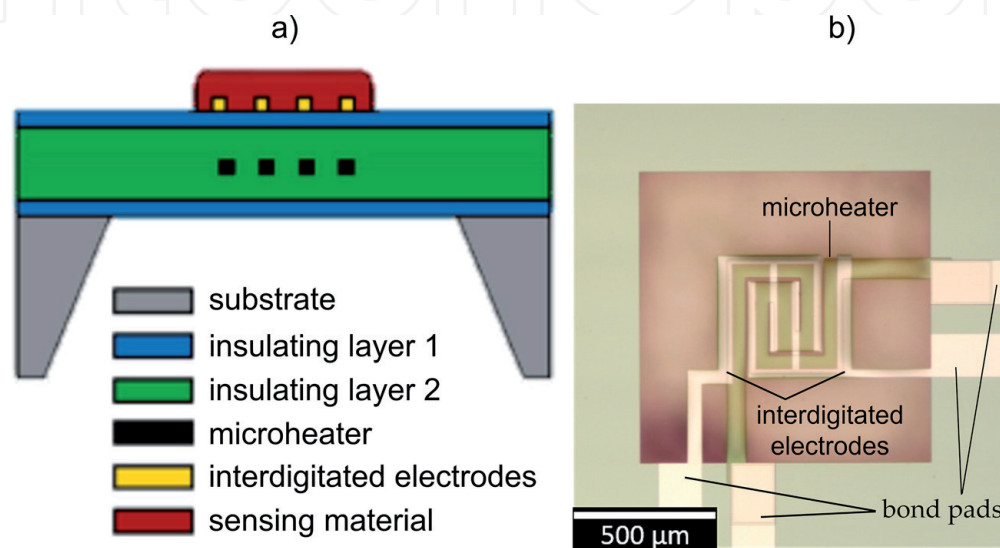


**Figure 13.** (a) Layout of a typical microresistor (lateral view); adapted with permission from [6], Copyright 2018 Authors, licensee MDPI. (b) Optical image of a microhotplate and its indicated components (top view).

micro-electro-mechanical systems (MEMS) technology. This facilitates their integration as arrays in monolithic microchips as well as the incorporation of microheaters with low thermal losses (the so-called microhotplates) [5, 6, 74].

**Figure 13a)** displays the typical architecture of a microresistor consisting of a microhotplate and a sensing material on its top, and **Figure 13b)** shows an image of a microhotplate. This consists of a thin layer (a few micrometers thick) of a dielectric material, also called a membrane, supported by a silicon substrate at its periphery. The microheater is embedded within the membrane and insulated from the interdigitated electrodes patterned on top of the membrane. The use of silicon and MEMS technologies allows for the incorporation of integrated circuits along with the driving and signal conditioning circuitry or other smart features (e.g., wireless communication) to build electronic noses with potentially low-cost production [152, 153]. However, recently other substrate materials (e.g., polymers) and technologies (e.g., printing) are being explored and optimized to provide also integrated elements driven by the use of optimized active 1D MOS nanostructures that can operate at room temperature or close to it [13, 154].

#### 4.2 Assembly of 1D metal oxide nanostructures on transducer platforms

To enable practical use of 1D MOS nanostructures, these structures must bring the interdigitated electrodes (chemiresistor) or the source and drain electrodes (FET) into contact. This allows the electrical current to flow and the resistance (or

conductance) changes to be monitored. Such connection can be attained either by a single 1D nanostructure or by multiple 1D nanostructures [52, 54, 98]. Due to the requirement of precise alignment between the 1D nanostructure and the patterned electrodes, the fabrication process of the individual 1D nanostructure device is rather complicated, time-consuming and expensive. Therefore, to simplify the fabrication process and electrical signal measurement, the multiple 1D nanostructure devices become the most widely accepted configuration for practical applications.

#### 4.2.1 Coating methods

The assembly of multiple 1D nanostructures for chemical sensors usually involves the use of a two-step process [52], following any of the routes sketched in **Figure 14a**). In the first route (top-electrode architecture), either 1D nanostructures are synthesized directly on a blank substrate or pre-synthesized 1D nanostructures are transferred on the substrate. Then, the electrodes are deposited by sputtering on the substrate with the 1D nanostructures on their top with the help of a mask. Conversely, in the second route (bottom-electrode architecture), the electrodes are deposited firstly on the blank substrate and the 1D nanostructures are either synthesized or transferred on the substrate with the patterned electrodes on its top. Technologically, bottom-electrode architectures are preferred for chemical sensors, as they may facilitate the direct integration of 1D nanostructures. This type of architecture also prevents the introduction of contaminants into the sensitive materials as the processing steps for the definition of the electrode are performed before the integration of the sensitive material.

The synthesis of 1D MOS nanostructures directly onto the sensor substrate [155], either a blank substrate or a substrate with patterned electrodes, is the preferred choice, since it reduces the fabrication time and costs of the sensors. Also, it reduces the incorporation of contaminants by avoiding the use of transfer media (often liquids) that tend to degrade the surface properties of the sensitive structures. On the other hand, the direct integration of 1D MOS nanostructures demands substrate materials such as silicon (Si), alumina ( $\text{Al}_2\text{O}_3$ ), quartz, or high-temperature-resistant polymers (e.g., polyimide PI) [156] capable to withstand the thermal steps required for the synthesis of the MOS nanostructures and the

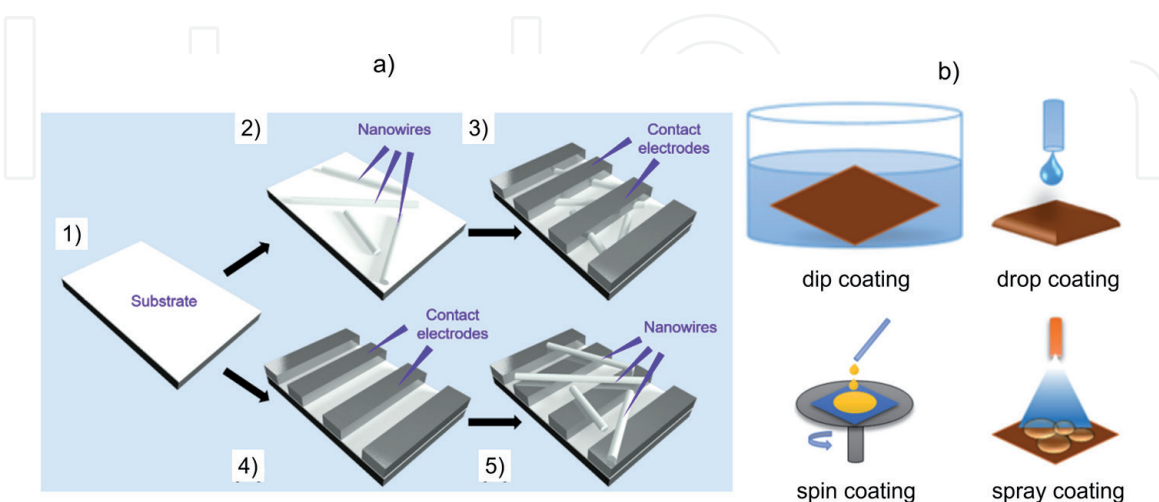


**Figure 14.**

(a) Schematic diagram of the architectures (top- or bottom-electrodes) used in multiple 1D nanostructures based chemical sensors: (1) blank substrate, (2) nanowires transferred onto the blank substrate, (3) electrodes patterned onto the substrate with nanowires, (4) electrodes patterned onto the blank substrate, (5) nanowires transferred onto the substrate with patterned electrodes; adapted with permission from [52], Copyright 2021 Authors, licensee MDPI. (b) Schematic illustration of wet-coating methods for the transfer of nanomaterials from a liquid dispersion to a substrate; adapted from [158].

high operating temperatures of the MOS chemical sensors (>200 °C). However, since the most advanced functional nanomaterials for chemical sensing based on MOS suggest that the next generation of MOS chemical sensors could work at room temperature, the need for heating elements could be omitted in the future, opening the possibility to use more abundant substrate materials that are cheaper and easier to process compared to those above. In this respect, steps are already being taken towards the synthesis of 1D MOS nanostructures on tiny substrates of flexible stretchable soft polymers (e.g., polyethylene terephthalate PET, polytetrafluoroethylene PTFE, polyaniline PANI, polyimide PI), textiles, or paper [157], which are of major interest for use in wearable sensor devices for emerging applications (e.g., healthcare). To achieve this, the processing temperatures are required to be below the glass transition temperature of polymers (<400 °C PI) or the thermal degradation temperature of the substrates (<100 °C textiles, paper). This limits the application of some synthetic procedures as those based on high-temperature chemical vapor deposition or electrospinning, as they demand temperatures of at least 400°C for either precursor decomposition or sintering steps. Then, the transfer of the pre-synthesized 1D nanostructures on flexible substrates seems to be the only feasible alternative to date.

The transfer of the pre-formed 1D MOS nanostructures to the sensor substrate may be a complex, time-consuming and expensive approach. In transfer methods, firstly, the 1D nanostructures need to be detached from the substrate on which they were synthesized and subsequently be dispersed in a liquid, usually a volatile organic solvent. There is a diversity of wet-coating techniques to transfer nanomaterials in suspension in a liquid to a substrate. The most common ones are illustrated in **Figure 14b**) [158]. Basically, the choices are either immersing the sensor substrate in the dispersion (dip-coating) or dosing the dispersion in form of droplets (drop coating, spin coating, spray coating) that settle on the substrate. The liquid evaporates from the in-flight droplets and/or the substrate, which can be heated at a constant temperature during or at the end of the transfer process.

The two approaches described previously result in multiple 1D MOS nanostructures forming a mat- or web-like deposit; this is a stacked network of 1D MOS nanostructures lying randomly in all directions of space. The deposits often display a bi-modal pore size distribution with relatively large pores (sub-micron to a few microns) side by side with nanosized pores (e.g., electrospun nanofibers), facilitating effective gas transport into the sensing layer. In addition, there are many cross-points between the 1D nanostructures in the network, which may favor the current percolation and the whole conductivity of the film. Nevertheless, several weaknesses have been identified in these mat-type sensitive layers that bring into question their usefulness for chemical sensors.

Even if the above techniques allow for a high degree of control of the parameters relevant to the synthesis or transfer of the 1D nanostructures, properties such as the size, thickness, porosity, or nano/microstructure vary greatly from one deposit to another, which lead to differences in the chemical sensing performance between sensors. To overcome this problem, wire structures connected in parallel are the ideal architecture to achieve a well-defined conduction channel that is easy to modulate by the interactions of the analyte and surface. In such a structure the grain boundaries or nanowire-nanowire interfaces are removed and thus the sensitivity of the system depends only on the nanowire surface due to an efficient transfer of charge with a lower probability of recombination. Usual approaches to achieve such integration of 1D nanostructures involve alignment methods based on the Langmuir-Blodgett technique or electric and magnetic field-assisted orientation techniques [159] such as dielectrophoresis [160]. For instance, a recent report based on the dielectrophoresis method proposed the use of a nanoelectrode array

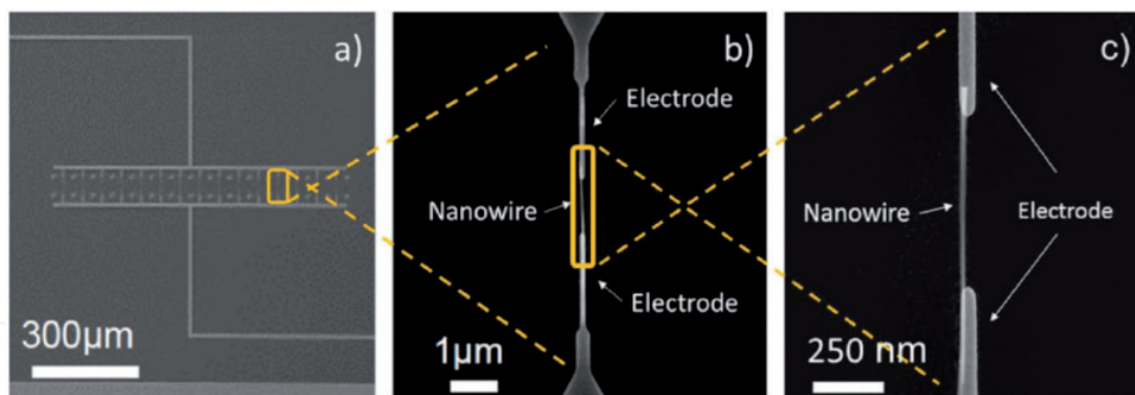


**Figure 15.**

(a) View of a nanoelectrode array containing several single-nanowires connected in parallel. (b), (c) Detailed views of a pair of nanoelectrodes with a nanowire interconnected across them; reprinted from [161].

system for the integration of various single-nanowires connected in parallel [161]. This system allowed for the selective integration of single-nanowires connected across various faced electrodes using the dielectrophoresis method, as can be observed in **Figure 15**.

Several methods have also been developed to orient and align electrospun fibers, either mechanically (e.g., rotating drum, rotating sharp disk) [84, 162–164] or by the action of electric fields [165–167]. In the latter, gaps of an insulating material (e.g., air, quartz, polystyrene) are introduced on the surface of a conductive substrate, and patterned electrodes (e.g., interdigitated electrodes) can also be used to obtain oriented nanofibers. When an insulating gap is introduced into the collector, it changes the structure of the external electric field. As a result, the directions of the electrostatic forces acting on a fiber that is sitting across the gap will be altered. In addition, once the charged fiber has moved into the vicinity of the electrodes, charges on the fiber will induce opposite charges on the surface of the electrodes. These opposite charges will further attract the fiber to the electrodes. These two types of electrostatic forces simultaneously pull the fiber towards the edge of the two electrodes and acting on different portions of a fiber will eventually lead to its uniaxial alignment through the gap, as can be seen in **Figure 16** [167].

It has been observed that the electrospun MOS nanofibers have a weak interfiber interaction and poor adherence to the electrodes and the substrate, resulting in high contact resistance and inferior mechanical properties. Thus, various treatments have been applied to the as-spun polymer/inorganic precursor fibers before sintering. These are traditional treatments such as irradiation with UV-light [168] or hot-pressing [169, 170], and a novel nanoscale welding technique [171]. The latter is simple and easy to apply, does not require specific equipment, preserves the interconnected structure of nanofibers, and is also the most efficient in terms of enhancement of the interfiber connections and interfacial adhesion. All this makes it the optimal treatment for application in chemical sensors.

Usually, conventional wet-coating techniques do not allow for highly-localized highly-dispersed coating of very small areas. Ideally, the sensing material should cover only the zone spanned by the electrodes, this is the active surface of the sensor whose area in the case of the microsensors is typically less than  $0.2 \text{ mm}^2$ . In practice, however, it is necessary to use masks to keep the region around the electrodes clean, particularly the bond pads of the electrodes and microheater. In this regard, the electrohydrodynamic jet printing technique [172–174], also called e-jet printing, is a precise way to transfer nanomaterials in a liquid on a substrate with greater resolution and repeatability than standard wet-coating and printing techniques (e.g., screen printing, aerosol-jet printing, ink-jet printing). In e-jet printing,

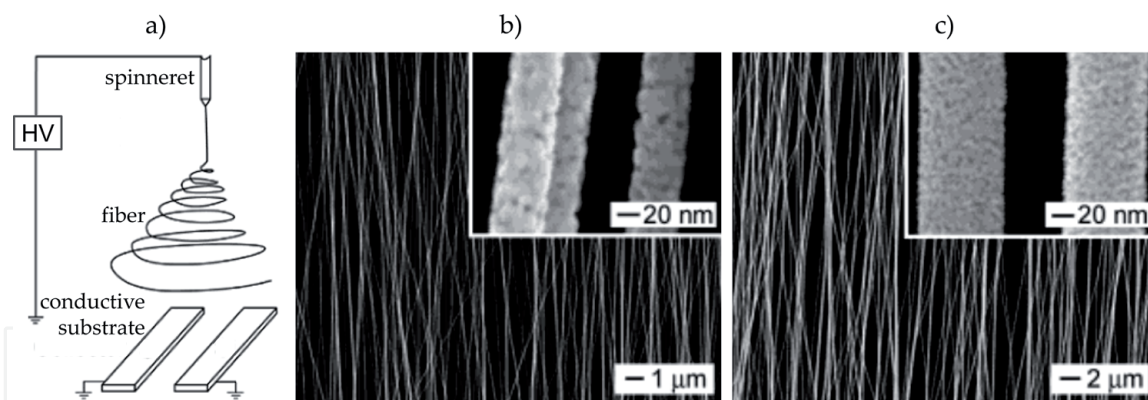


**Figure 16.** (a) Layout of the setup to electrospin fibers as uniaxially aligned arrays, where the collector consists of two conductive strips separated by a void gap. SEM micrographs of uniaxially aligned electrospun nanofibers of (b)  $\text{TiO}_2$  and (c)  $\text{Sb}$ -doped  $\text{SnO}_2$ ; the insets show enlarged SEM micrographs of the nanofibers. Adapted with permission from [167], Copyright 2003 American Chemical Society.

droplets of a liquid suspension, also called an ink, are pulled out from a nozzle by the action of an external electric field. Charges accumulate at the liquid surface and the coulombic repulsion causes the liquid meniscus at the nozzle tip to deform into a conical shape (Taylor cone). When the electric field exceeds a critical value, the stress from the surface charge repulsion at the cone apex exceeds the surface tension and a small droplet is emitted towards the substrate. The key to high-resolution droplet printing is to use electric potentials below those required for droplet atomization (electrospray) and small nozzles ( $<100 \mu\text{m}$ ). Then, the deposited droplets can be as small as hundreds of nanometers.

Highly integrated arrays of MEMS gas sensors have been prepared by e-jet printing [175, 176], as depicted in **Figure 17**. Firstly, long electrospun MOS nanofibers were fragmented into smaller pieces by ultrasonication and dispersed in a liquid. The electrodes were then coated with the fragments of the MOS nanofibers by using an e-jet printing system including a pulse-modulated voltage supply and a moving stage to control the droplet size and droplet position, respectively. The nozzle used was less than  $100 \mu\text{m}$  in inner diameter and the dot pattern size of the MOS nanofibers was in the order of  $40\text{--}60 \mu\text{m}$ . It is worth mentioning that e-jet printing was accomplished without nozzle clogging and that all the microsensors survived the process, in contrast to the standard wet-coating techniques, where the failure of the microsensor is frequently observed owing to the impact of big droplets, typically of tens of micrometers, causing the fragile dielectric membrane to crack. Furthermore, using a smaller nozzle, adjusting the applied voltage and pulse width, and tightly controlling the X-Y moving platform a continuous jetting regime was

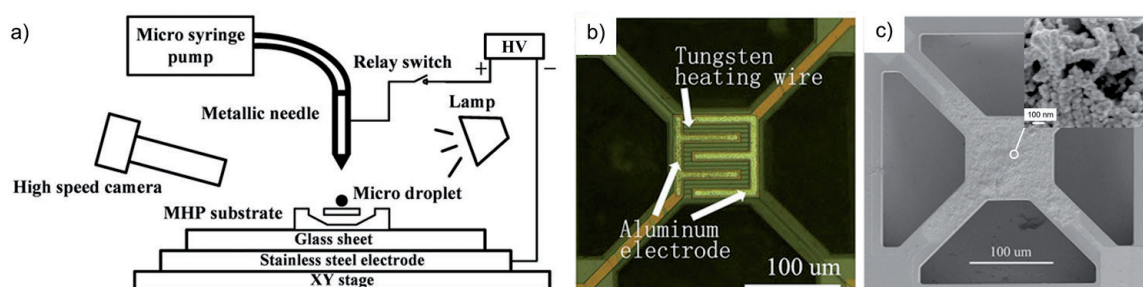


**Figure 17.** (a) Layout of a typical setup for e-jet printing mounted on an X-Y positioning stage, (b) Optical microscope micrograph of the microhotplate (MHP), (c) SEM micrograph of the MHP coated with fragments of  $\text{Pd}$ -loaded  $\text{SnO}_2$  nanofibers (inset) by using the e-jet printing setup in (a). Adapted with permission from [175], Copyright 2018 Authors.

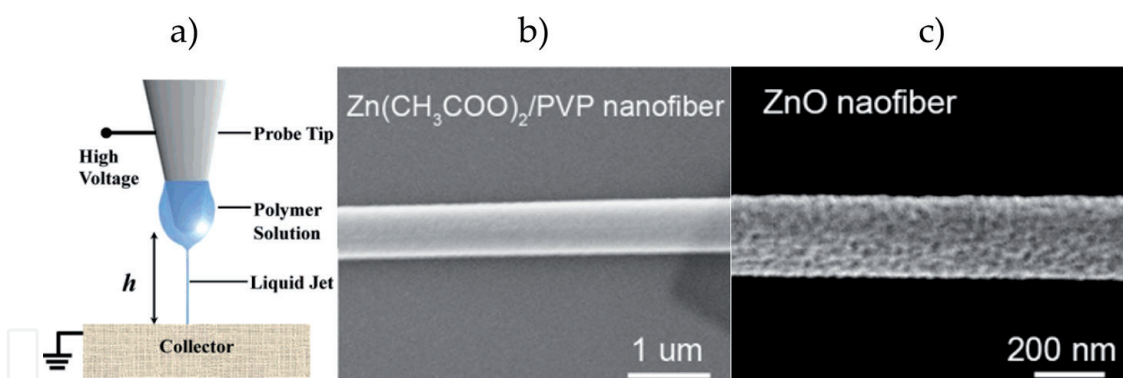


**Figure 18.**

(a) Sketch of a typical electrohydrodynamic direct-writing (EDW) setup; reprinted with permission from [186], Copyright 2006 American Chemical Society. SEM images of (b) PVP/Zn fiber obtained by EDW over a silicon substrate and (c) ZnO nanofiber obtained by sintering of the PVP/Zn fiber in (b); reprinted with permission from [189], Copyright 2013 Elsevier.

achieved, enabling to print line patterns less than  $40\mu\text{m}$  in width with a maintained geometry and homogeneous distribution of the fragments of MOS nanofibers [176].

#### 4.2.2 Patterning methods

Conventional methods based on micro- and nano-fabrication top-down processes that include steps of deposition, lithography, and etching may be used to pattern 1D MOS nanostructures and assist the growth of 1D MOS nanostructures in selected areas of a device. These processes are usually employed to define the area, density, and size of 1D nanostructures by patterning catalyst seeds that assist the growth of 1D nanostructures via VLS growth mechanisms. Other approaches also include forming templates to assist the directional growth of 1D nanostructures with subsequent template etching to free the 1D nanostructures. Hence, these processes generally lead to vertical aligned 1D nanostructures that are bridged with top and bottom contact as resistors or as FETs, for instance, by adding a vertical surrounded-gate [177, 178]. These approaches are not discussed in this chapter and more details can be found in the following literature [55, 158, 179, 180].

The electrospinning technique is more suited for the formation of nanofiber mats on areas that largely exceed the active area of the chemical sensors. Generally, the size of the area covered with the electrospun fibers decreases with the decreasing nozzle-to-substrate distance, which is accompanied by a reduction of the applied potential to preserve the electric field and prevent the onset of electrical discharges. The near-field electrospinning (NFES) method, also known as the electrohydrodynamic direct-writing (EDW) method, exploits this behavior [181–186]. The working principle of EDW is similar to that of the traditional electrospinning but with some distinctive features, namely the small nozzle diameter ( $<50\mu\text{m}$ ), the low applied voltage ( $<1\text{ kV}$ ), the short distance between the nozzle and the substrate (0.5–5 mm), and the use of a moving nozzle and/or substrate, which facilitates position-tunable alignment and on-demand patterning of fibers on the substrate. EDW uses the stability region of the liquid jet and supplies discrete droplets of the polymer solution, in the same way as a dip pen does. This technique has been proven for direct-writing individual MOS nanofibers on silicon substrate for use in both chemiresistive [187, 188] and FET [189] sensor devices. As an example, **Figure 18** shows images of a ZnO nanofiber obtained by sintering a PVP/Zn nanofiber written by EDW on a substrate.

## 5. Summary and outlook

This chapter provides a general overview of the status and recent advances in developing chemical sensors based on 1D MOS nanostructures. The contents focus on the most frequent strategies and methods used to achieve higher sensing performances to cope with present and future applications, which ultimately drive innovation in chemical sensors. The applications usually impose requirements in terms of capabilities and efficiency of chemical detection, miniaturization, fabrication costs, power consumption, sensor stability, and lifetime. The combination of these needs poses difficult challenges to a diversity of enabling technologies encompassing materials synthesis, nanotechnology, nano- and micro-fabrication, and printing technologies, amongst others. In this context, the survey covers the state-of-the-art and advances of the main synthetic methods to produce 1D sensitive materials used in chemical sensors, particularly, nanowires and nanofibers based on MOS. It also tackles the effect of incorporating second-phase materials to bring improved and/or new chemical sensing attributes to single-phase 1D MOS nanostructures and the routes to form this type of heteronanostructures. Finally, it discusses the most common chemical sensing architectures to enable the response of 1D nanostructures via resistive or FET measurements, as well as the techniques used to assemble the nanostructures onto these sensor platforms (of resistive and FET type).

The vast reports and prospects in chemical sensors indicate that the trends of these devices are directed towards further miniaturization and operation at the minimum power consumption. The last will be achieved mainly by reducing the operating temperature (at which sensitive MOS materials are stimulated) to levels close to room temperature. Improvements on traditional functional parameters such as the sensitivity, stability, speed of response, and selectivity to application-dependent target analytes are also expected. All these improvements may ultimately come true by gaining a better understanding of the synergistic sensing effects in 1D heteronanostructures composed of MOS, metals and/or 2D nanomaterials such as graphene, TMDC, or MXenes. So that these combinations can be tailored more precisely shortening the try and error steps currently employed when tuning sensitive heteronanostructures. Certainly, this knowledge needs to be developed in parallel to robust and reproducible routes to synthesize 1D MOS heteronanostructures. The new synthetic routes must be optimized to enable the high dispersion, homogeneous distribution, and maximal interfacial area between the MOS and the second-phase constituents, with the minimum penalty in terms of sustainability, cost-effectiveness, and scalability. One-step routes that allow to grow, form, or assemble 1D MOS nanostructures directly onto the transducer platforms are pursued in the first place, followed by the techniques that allow the transfer of pre-formed 1D MOS nanostructures onto the transducer platforms with good control over the nanostructure orientation, alignment, and electrical contacts. When applied to the fabrication of chemical sensors, both types of techniques need to ensure the localized integration of 1D MOS nanostructures over the active area of the sensor device. This means that direct and transfer methods for the integration of 1D nanostructures must be adapted to operate efficiently either, in small sensitive areas, in agreement with the materials used as platforms, for instance, silicon-based MEMS or temperature-sensitive substrates (polymers, textiles, etc.). Therefore, the integration methods must also ensure control in the sub-millimeter range, optimal connectivity and conductivity between the nanostructures bridging the interdigitated electrodes, and strong adhesion of the nanostructures to the transducer platform.

Traditional synthetic methods based on nucleation and growth processes, such as hydrothermal synthesis and chemical vapor deposition, must be exploited to allow one-step integration of 1D MOS nanostructures with transducer platforms. These techniques are appropriate for direct integration, particularly with silicon-based platforms. However, their potential is not fully exploited as most of the works on chemical sensors fabrication turn to a removal and re-deposition approach for integrating 1D MOS nanostructures synthesized by these techniques.

The electrohydrodynamic techniques emerge as a promising alternative for integrating 1D MOS nanostructures onto chemiresistive and FET platforms due to its high-precision for printing areas of less than  $0.1 \text{ mm}^2$  (e-jet printing) or its high-resolution to write directly (on electrodes and substrate patterns) lines of less than 100 nm in width. The direct printing of 1D MOS nanostructures may improve the reproducibility of chemical sensors. The application of electrohydrodynamic techniques to manufacture chemical sensors using MOS is still at an early stage. Much effort needs to be done to optimize the composition and properties of the dispersion and polymer solutions (inks), nozzle geometry and dimensions, and process conditions, before these techniques, become a rapid and cost-effective tool for large-scale fabrication of chemical sensors based on MOS. However, their availability in the short term could push forward the application of 1D nanostructures and emerging flexible substrates for chemical sensors.

## Acknowledgements

The programme Interreg V Sudoe of the EU (Grant SEO2/P1/E569, NanoSen-AQM) is acknowledged for funding this publication. SV acknowledges the support of MCIN/AEI/10.13039/501100011033, via Grant PID2019-107697RB-C42 (ERDF A way of making Europe).

## Author details

Esther Hontañón<sup>1\*</sup> and Stella Vallejos<sup>2</sup>

<sup>1</sup> Institute of Physical and Information Technologies, Spanish National Research Council, Madrid, Spain

<sup>2</sup> Institute of Microelectronics of Barcelona, Spanish National Research Council, Cerdanyola del Vallès, Barcelona, Spain

\*Address all correspondence to: esther.hontanon@csic.es

## IntechOpen

© 2021 The Author(s). Licensee IntechOpen. This chapter is distributed under the terms of the Creative Commons Attribution License (<http://creativecommons.org/licenses/by/3.0>), which permits unrestricted use, distribution, and reproduction in any medium, provided the original work is properly cited. 

## References

- [1] Gomes JB, Rodrigues JJPC, Rabêlo RAL, Kumar N, Kozlov S. IoT-enabled gas sensors: Technologies, applications and opportunities. *Journal of Sensors and Actuators Networks*. 2019;**8**:29. DOI: 10.3390/jsan8040057
- [2] Wang H, Ma J, Zhang J, Feng Y, Vijjapu MT, Yuvaraja S, et al. Gas sensing materials roadmap. *Journal of Physics: Condensed Matter*. 2021;**33**:303001. DOI: 10.1088/1361-648X/abf477
- [3] Saruhan B, Fomekong RL, Nahirniak S. Review: Influences of semiconductor metal oxide properties on gas sensing characteristics. *Frontiers in Sensors*. 2021;**2**:657931. DOI: 10.3389/fsens.2021.657931
- [4] Serban I, Enesca A. Metal oxides-based semiconductors for biosensors applications. *Frontiers in Chemistry*. 2020;**8**:354. DOI: 10.3389/fchem.2020.00354
- [5] Briand D, Courbat J. Micromachined semiconductor gas sensors. In: Jaaniso R, Tan OK, editors. *Semiconductor Gas Sensors*. Woodhead Publishing Series in Electronic and Optical Materials. 2nd ed. Amsterdam: Elsevier; 2020. pp. 413-464. DOI: 10.1016/B978-0-08-102559-8.00013-6
- [6] Liu H, Zhang L, Li KHH, Tan OK. Microhotplates for metal oxide semiconductor gas sensor applications-Towards the CMOS-MEMS monolithic approach. *Micromachines*. 2018;**9**:557. DOI: 10.3390/mi9110557
- [7] Korotcenkov G. Gas response control through structural and chemical modification of metal oxide films: State of the art and approaches. *Sensors and Actuators B*. 2005;**107**:209-232. DOI: 10.1016/j.snb.2004.10.006
- [8] Park SY, Kim Y, Kim T, Eom TH, Kim SY, Jang HW. Chemoresistive materials for electronic nose: Progress, perspectives, and challenges. *InfoMat*. 2019;**1**(7):289-316. DOI: 10.1002/inf2.12029
- [9] Schütze A, Sauerwald T. Dynamic operation of semiconductor sensors. In: Jaaniso R, Tan OK, editors. *Semiconductor Gas Sensors*. Woodhead Publishing Series in Electronic and Optical Materials. 2nd ed. Amsterdam: Elsevier; 2020. pp. 385-412. DOI: 10.1016/B978-0-08-102559-8.00012-4
- [10] Palacio F, Fonollosa J, Burgués J, Gomez JM, Marco S. Pulsed-temperature metal oxide gas sensors for microwatt power consumption. *IEEE Access*. 2020;**8**:70938-70946. DOI: 10.1109/ACCESS.2020.2987066
- [11] Kumar R, Liu X, Kumar M. Room-temperature gas sensors under photoactivation: From metal oxides to 2D materials. *Nano-Micro Letters*. 2020;**12**:164. DOI: 10.1007/s40820-020-00503-4
- [12] Majhi SM, Mirzaei A, Kim HW, Kim SS, Kim TW. Recent advances in energy-saving chemiresistive gas sensors: A review. *Nano Energy*. 2021;**79**:105369. DOI: 10.1016/j.nanoen.2020.105369
- [13] Dai J, Ogbeide O, Macadam N, Sun Q, Yu W, Li Y, et al. Printed gas sensors. *Chemical Society Reviews*. 2020;**49**:1756-1789. DOI: 10.1039/c9cs00459a
- [14] Fazio E, Spadaro S, Corsaro C, Neri G, Leonardi SG, Neri F, et al. Metal-oxide based nanomaterials: Synthesis, characterization and their applications in electrical and electrochemical sensors. *Sensors*. 2021;**21**:2494. DOI: 10.3390/s21072494
- [15] Naresh V, Lee N. A review on biosensors and recent development of

- nanostructured materials-enabled biosensors. *Sensors*. 2021;**21**:1109. DOI: 10.3390/s21041109
- [16] Wang Z, Zhu L, Sun S, Wang J, Yan W. One-dimensional nanomaterials in resistive gas sensor: From material design to application. *Chemosensors*. 2021;**9**:198. DOI: 10.3390/chemosensors9080198
- [17] Malik R, Towner VK, Mishra YK, Lin L. Functional gas sensing nanomaterials: A panoramic view. *Applied. Physics Reviews*. 2020;**7**:021301. DOI: 10.1063/1.5123479
- [18] Nunes D, Pimentel A, Goncalves A, Pereira S, Branquinho R, Barquinha P, et al. Metal oxide nanostructures for sensor applications. *Semiconductor Science and Technology*. 2019;**34**:043001. DOI: 10.1088/1361-6641/ab011e
- [19] Qadir A, Le TK, Malik M, Min-Dianey KAA, Saeed I, Yu Y, et al. Representative 2D-material-based nanocomposites and their emerging applications: A review. *RCS Advances*. 2021;**11**:23860-23880. DOI: 10.10139/d1ra03425a
- [20] Pham VP, Nguyen MT, Park JW, Kwak SS, Nguyen DHT, Mun MK, et al. Chlorine-trapped CVD bilayer graphene for resistive pressure sensor with high detection limit and high sensitivity. *2D Materials*. 2017;**4**(2):025049. DOI: 10.1088/2053-1583/aa6390
- [21] Chen X, Leishman M, Bagnall D, Nasiiri N. Nanostructured gas sensors: From air quality and environmental monitoring to healthcare and medical applications. *Nanomaterials*. 2021;**11**:1927. DOI: 10.3390/nano11081927
- [22] Kumar DK, Reddy KR, Sadhu V, Shetti NP, Reddy CV, Chouhan RS, et al. Metal oxide-based nanosensors for health care and environmental applications. In: Kanchi S, Sharma D, editors. *Nanomaterials in Diagnostic Tools and Devices*. 1st ed. Amsterdam: Elsevier; 2020. pp. 113-129. DOI: 10.1016/C2018-0-02240-9
- [23] Xue S, Cao S, Huang Z, Yang D, Zhang G. Improving gas-sensing performance based on MOS nanomaterials: A review. *Materials*. 2021;**14**:4263. DOI: 10.3390/ma14154263
- [24] Sun Z, Liao T, Kou L. Strategies for designing metal oxide nanostructures. *Science China Materials*. 2017;**60**:1. DOI: 10.1007/s40843-016-5117-0
- [25] Yang B, Myung NV, Tran T-T. 1D metal oxide semiconductor materials for chemiresistive gas sensors: A review. *Advanced Electronic Materials*. 2021;**7**:2100271. DOI: 10.1002/aelm.202100271
- [26] Kaur N, Singh M, Comini E. One-dimensional nanostructured chemoresistive sensors. *Langmuir*. 2020;**36**:6326-6344. DOI: 10.1021/acs.langmuir.0c00701
- [27] Hulanicki A, Glab S, Ingman F. Chemical sensors definitions and classification. *Pure and Applied Chemistry*. 1991;**63**(9):1247-1250. DOI: 10.1351/pac199163091247
- [28] Deng Y. Sensing mechanism and evaluation criteria of semiconducting metal oxides gas sensors. In: *Semiconducting Metal Oxides for Gas Sensing*. 1st ed. Singapore: Springer Nature; 2019. pp. 23-51. DOI: 10.1007/978-981-13-5853-1
- [29] Korotcenkov G. Metal oxides for solid-state gas sensors: What determines our choice? *Materials Science and Engineering B*. 2007;**139**:1-23. DOI: 10.1016/j.mceb.2007.01.044
- [30] Kim H-J, Lee J-H. Highly sensitive and selective gas sensors using p-type oxide semiconductors: Overview. *Sensors and Actuators B*. 2014;**192**:607-627. DOI: 10.1016/j.snb.2013.11.005

- [31] Annanouch FE, Haddi Z, Vallejos S, Umek P, Guttman P, Bittencourt C, et al. Aerosol-assisted CVD-grown WO<sub>3</sub> nanoneedles decorated with copper oxide nanoparticles for the selective and humidity-resilient detection of H<sub>2</sub>S. *ACS Applied Materials & Interfaces*. 2015;7:6842-6851. DOI: 10.1021/acsami.5b00411
- [32] Choopun S, Hongsith N, Wongrat E. Metal oxide nanowires for gas sensors. In: Peng X, editor. *Nanowires—Recent Advances*. London: IntechOpen; 2012. pp. 3-23. DOI: 10.5772/54385
- [33] Vergara A, Llobet E. Sensor selection and chemo-sensory optimization: Toward an adaptable chemo-sensory system. *Frontiers in Neuroengineering*. 2012;4:19. DOI: 10.3389/fneng.2011.00019
- [34] Gurlo A. Nanosensors: Towards morphological control of gas sensing activity. SnO<sub>2</sub>, In<sub>2</sub>O<sub>3</sub>, ZnO and WO<sub>3</sub> case studies. *Nanoscale*. 2011;3:154-165. DOI: 10.1039/C0NR00560F
- [35] Li Z, Li H, Wu Z, Wang M, Luo J, Torun H, et al. Advances in designs and mechanisms of semiconducting metal oxide nanostructures for high-precision gas sensors operated at room temperature. *Materials Horizon*. 2019;6:470-506. DOI: 10.1039/c8mh01365a
- [36] Yang S, Lei G, Xu H, Lan Z, Wang Z, Gu H. Metal oxide based heterojunctions for gas sensors: A review. *Nanomaterials*. 2021;11:1026. DOI: 10.3390/nano11041026
- [37] Sadighbayan D, Hasanzadeh M, Ghafar-Zadeh E. Biosensing based on field-effect transistors (FET): Recent progress and challenges. *Trends in Analytical Chemistry*. 2020;133:116067. DOI: 10.1016/j.trac.2020.116067
- [38] Joshi N, Baunger ML, Shimiziu FM, Riul A, (Jr), Oliveira O N (Jr). Insights into nano-heterostructured materials for gas sensing. A review. *Multifunctional Materials*. 2021;4(3): 032002. DOI: 10.1088/2399-7532/ac1732
- [39] Walker JM, Akbar SA, Morris PA. Synergistic effects in gas sensing semiconducting oxide nano-heterostructures: A review. *Sensors and Actuators B*. 2019;286:624-640. DOI: 10.1016/j.sintl.2019.01.049
- [40] Deng Y. Semiconducting metal oxides: Composition and sensing performance. In: *Semiconducting Metal Oxides for Gas Sensing*. 1st ed. Singapore: Springer Nature; 2019. pp. 77-103. DOI: 10.1007/978-981-13-5853-1
- [41] Zappa D, Galstyan V, Kaur N, Arachchige HMMM, Sisman O, Comini E. Metal oxide-based heterostructures for gas sensors—A review. *Analytical Chimica Acta*. 2018;1039:1-23. DOI: 10.1016/j.aca.2018.09.020
- [42] Miller DR, Akbar SA, Morris PA. Nanoscale metal oxide-based heterojunctions for gas sensing: A review. *Sensors and Actuators B*. 2014;204:250-272. DOI: 10.1016/j.snb.2014.07.074
- [43] Tobaldi DM, Leonardi SG, Movlaee K, Lajaunie L, Seabra MP, Arenal R, et al. Hybrid noble metals/metal-oxide bifunctional nano-heterostructure displaying outperforming gas-sensing and photocromic performances. *ACS Omega*. 2018;3:9846-9859. DOI: 10.1021/acsomega.8b01508
- [44] Müller SA, Degler D, Feldmann C, Türk M, Moos R, Fink K, et al. Exploiting synergies in catalysis and gas sensing using noble metal-loaded oxide composites. *ChemCatChem*. 2018;10: 864-880. DOI: 10.1002/cctc.201701545
- [45] Rai P, Majhi SM, Yu Y-T, Lee J-H. Noble metal@metal oxide semiconductor core@shell nano-architectures as a new

- platform for gas sensors applications. *RCS Advances*. 2015;5:76229-76248. DOI: 10.1039/c5ra14322e
- [46] Jian Y, Hu W, Zhao Z, Cheng P, Haick H, Yao M, et al. Gas sensors based on chemi-resistive hybrid functional nanomaterials. *Nano-Micro Letters*. 2020;12:71. DOI: 10.1007/s40820-020-0407-5
- [47] Sowmya B, John A, Panda PK. A review on metal-oxide based p-n and n-n heterostructured nano-materials for gas sensing applications. *Sensors International*. 2021;2:100085. DOI: 10.1016/j.sintl.2021.100085
- [48] Sun D, Luo Y, Debliquy M, Zhang C. Graphene-enhanced metal oxide gas sensors at room temperature: A review. *Beilstein Journal of Nanotechnology*. 2018;9:2832-2844. DOI: 10.3762/bjnano.9.264
- [49] Aroutiounian VM. Metal oxide gas sensors decorated with carbon nanotubes. *Lithuanian Journal of Physics*. 2015;55(4):319-329. DOI: 10.3952/physics.v55i4.3230
- [50] Bhati VS, Kumar M, Banerjee R. Gas sensing performance of 2D nanomaterials/metal oxide nanocomposites: A review. *Journal of Materials Chemistry C*. 2021;9:8776-8808. DOI: 10.1039/d1tc01857d
- [51] Li Z, Yao Z, Haidry AA, Plecenik T, Xie L, Sun L, et al. Resistive-type hydrogen gas sensor based on TiO<sub>2</sub>: A review. *International Journal of Hydrogen Energy*. 2018;43:21114-21132. DOI: 10.1016/j.ijhydene.2018.09.051
- [52] Zeng H, Zhang G, Nagashima K, Takahashi T, Hosomi T, Yanagida T. Metal-oxide nanowire molecular sensors and their promises. *Chemosensors*. 2021;9:41. DOI: 10.3390/chemosensors9020041
- [53] Wang F, Zu H. Application of one-dimensional metal oxide semiconductor in field effect transistor. In: Zhou Y, editor. *Semiconducting Metal Oxide Thin Film Transistors*. 1st ed. Bristol: IOP Publishing; 2021. pp. 6-1-6-25. DOI: 10.1088/978-0-7503-2556-1ch6
- [54] Korotcenkov G. Current trends in nanomaterials for metal oxide-based conductometric gas sensors: Advantages and limitations. Part 1: 1D and 2D nanostructures. *Nanomaterials*. 2020;10:1392. DOI: 10.3390/nano10071392
- [55] Wang Y, Duan L, Deng Z, Liao J. Electrically transduced gas sensors based on semiconducting metal oxide nanowires. *Sensors*. 2020;20:6781. DOI: 10.3390/s20236781
- [56] Aliheidari N, Aliahmad N, Agarwal M, Dalir H. Electrospun nanofibers for label-free sensor applications. *Sensors*. 2019;19:3587. DOI: 10.3390/s19163587
- [57] Comini E. Metal oxide nanowire chemical sensors: Innovation and quality of life. *Materials Today*. 2016;10(10):559-567. DOI: 10.1016/j.mattod.2016.05.016
- [58] Comini E, Baratto C, Faglia G, Ferroni M, Ponzoni A, Zappa D, et al. Metal oxide nanowire chemical and biochemical sensors. *Journal of Materials Research*. 2013;28(21):2911-2931. DOI: 10.1557/jmr.2013.304
- [59] Ding B, Wang M, Wang X, Yu J, Sun G. Electrospun nanomaterials for ultrasensitive sensors. *Materials Today*. 2010;13(11):16-27. DOI: 10.1016/S1369-7021(10)70200-5
- [60] Comini E, Sberveglieri G. Metal oxide nanowires as chemical sensors. *Materials Today*. 2010;13(7-8):36-44. DOI: 10.1016/S1369-7021(10)70126-7
- [61] Lockman Z, editor. *1-Dimensional Metal Oxide Nanostructures: Growth,*

- Properties and Devices. 1st ed. Zhang S, editor. *Advances in Materials Science and Engineering*. Boca Raton: CRC Press Taylor & Francis Group; 2020. p. 347. DOI: 10.1201/9781351266727
- [62] Devan RS, Patil RA, Lin J-H, Ma Y-R. One-dimensional metal-oxide nanostructures: Recent developments in synthesis, characterization, and applications. *Advanced Functional Materials*. 2012;**22**:3326-3370. DOI: 10.1002/adfm.201201008
- [63] Comini E, Baratto C, Faglia G, Ferroni M, Vomiero A, Sberveglieri G. Quasi-one dimensional metal-oxide semiconductors: Preparation, characterization and application as chemical sensors. *Progress in Materials Science*. 2009;**54**:1-67. DOI: 10.1016/j.pmatsci.2008.06.003
- [64] Vallejos S, Di Maggio F, Shujah T, Blackman C. Chemical vapour deposition of gas sensitive metal oxides. *Chemosensors*. 2016;**4**:4. DOI: 10.3390/chemosensors4010004
- [65] Feng S-H, Li G-H. Hydrothermal and solvothermal synthesis. In: Xu R, Xu Y, editors. *Modern Inorganic Synthetic Chemistry*. 2nd ed. Amsterdam: Elsevier; 2017. pp. 73-104. DOI: 10.1016/B978-0-444-63591-4.00004-5
- [66] Alshehri NA, Lewis AR, Pleydell-Pearce C, Maffei TGG. Investigation of the growth parameters of hydrothermal ZnO nanowires for scale up applications. *Journal of the Saudi Chemical Society*. 2018;**22**(5):538-545. DOI: 10.1016/j.jscs.2017.09.004
- [67] Chang P-C, Fan Z, Wang D, Tseng W-Y, Chiou W-A, Hong J, et al. ZnO nanowires synthesized by vapor trapping CVD method. *Chemistry of Materials*. 2004;**16**:5133-5137. DOI: 10.1021/cm049182c
- [68] Tonezzer M, Armellini C, Toniutti L. Sensing performance of electronic noses: A comparison between ZnO and SnO<sub>2</sub> nanowires. *Nanomaterials*. 2021;**11**:2773. DOI: 10.3390/nano11112773
- [69] Zhou JX, Yin Z. Raman spectroscopy and photoluminescence study of single-crystalline SnO<sub>2</sub> nanowires. *Solid State Communications*. 2006;**138**(5):242-246. DOI: 10.1016/j.ssc.2006.03.007
- [70] Nekita S, Nagashima K, Zhang G, Wang Q, Kanai M, Takahashi T, et al. Face-selective crystal growth of hydrothermal tungsten oxide nanowires for sensing volatile molecules. *ACS Applied Nano Materials*. 2020;**3**(10):10252-10260. DOI: 10.1021/acsanm.0c02194
- [71] Kaur N, Zappa D, Poli N, Comini E. Integration of VLS-grown WO<sub>3</sub> nanowires into sensing devices for the detection of H<sub>2</sub>S and O<sub>3</sub>. *ACS Omega*. 2019;**4**(15):16336-16343. DOI: 10.1021/acsomega.9b01792
- [72] Wang F, Dong A, Buhro WE. Solution-liquid-solid synthesis, properties, and applications of one-dimensional colloidal semiconductor nanorods and nanowires. *Chemical Reviews*. 2016;**116**:10888-10933. DOI: 10.1021/acs.chemrev.5b00701
- [73] Kolasinski KW. Catalytic growth of nanowires: Vapor-liquid-solid, vapor-solid-solid, solution-liquid-solid and solid-liquid-solid growth. *Current Opinion on Solid State and Materials Science*. 2006;**10**:182-191. DOI: 10.1016/j.cossms.2007.03.002
- [74] Vallejos S, Gràcia I, Chmela O, Figueras E, Hubálek J, Cané C. Chemoresistive micromachined gas sensors based on functionalized metal oxide nanowires: Performance and reliability. *Sensors and Actuators B*. 2016;**235**:525-534. DOI: 10.1016/j.snb.2016.05.102

- [75] Qi H, Glaser ER, Caldwell JD, Prokes SM. Growth of vertically aligned ZnO nanowire arrays using bilayered metal catalysts. *Journal of Nanomaterials*. 2012;**2012**:260687. DOI: 10.1155/2012/260687
- [76] Rackauskas S, Nasibulin AG. Nanowire growth without catalysts: Applications and mechanisms at the atomic scale. *ACS Applied Nano Materials*. 2020;**3**(8):7314-7324. DOI: 10.1021/acsnm.0c01179
- [77] Zhang Z, Wang Y, Li H, Yuan W, Zhang X, Sun C, et al. Atomic-scale observation of vapor-solid nanowire growth via oscillatory mass transport. *ACS Nano*. 2016;**10**(1):763-769. DOI: 10.1021/acsnano.5b05851
- [78] Rackauskas S, Jiang H, Wagner JB, Shandakov SD, Hansen TW, Kauppinen EI, et al. In situ study of noncatalytic metal oxide nanowire growth. *Nano Letters*. 2014;**14**(10):5810-5813. DOI: 10.1021/nl502687s
- [79] Oh SH, Chisholm MF, Kauffman Y, Kaplan WD, Luo W, Rühle M, et al. Oscillatory mass transport in vapor-liquid-solid growth of sapphire nanowires. *Science*. 2010;**330**(6003):489-493. DOI: 10.1126/science.1190596
- [80] Barhoum A, Pal K, Rahier H, Uludag H, Kim IS. Nanofibers as new-generation materials: From spinning and nano-spinning fabrication techniques to emerging applications. *Applied Materials Today*. 2019;**17**:1-35. DOI: 10.1016/j.apmt.2019.06.015
- [81] Gugulothu D, Barhoum A, Nerella R, Ajmer R, Bechelany M. Fabrication of nanofibers: Electrospinning and non-electrospinning techniques. In: Barhoum A, Bechelany M, Makhlof ASH, editors. *Handbook of Nanofibers. Part I: Fundamental Aspects, Experimental Setup, Synthesis, Properties and Characterization*. 1st ed. Switzerland: Springer Nature; 2019. pp. 45-77. DOI: 10.1007/978-3-319-53655-2\_6
- [82] Kailasa S, Reddy MSB, Maurya MR, Rani BG, Rao KV, Sadasivuni KK. Electrospun nanofibers: Materials, synthesis parameters, and their role in sensing applications. *Macromolecular Materials and Engineering*. 2021;**306**:2100410. DOI: 10.1002/mame.202100410
- [83] Alghoraibi I, Alomari S. Different methods for nanofiber design and fabrication. In: Barhoum A, Bechelany M, Makhlof ASH, editors. *Handbook of Nanofibers. Part I: Fundamental Aspects, Experimental Setup, Synthesis, Properties and Characterization*. 1st ed. Switzerland: Springer Nature; 2019. pp. 79-124. DOI: 10.1007/978-3-319-53655-2\_11
- [84] Homaeigohar S, Davoudpour Y, Habibi Y, Elbahri M. The electrospun ceramic hollow nanofibers. *Nanomaterials*. 2017;**7**:383. DOI: 10.3390/nano7110383
- [85] Chen Y, Lu W, Guo Y, Zhu Y, Lu H. Synthesis, characterization and photocatalytic activity of nanocrystalline first transition-metal (Ti, Mn, Co, Ni and Zn) oxide nanofibers by electrospinning. *Applied Sciences*. 2019;**9**:8. DOI: 10.3390/app9010008
- [86] Bagchi S, Brar R, Singh B, Ghanshyam C. Instability controlled synthesis of tin oxide nanofibers and their gas sensing properties. *Journal of Electrostatics*. 2015;**78**:68-78. DOI: 10.1016/j.elstat.2015.11.001
- [87] Li Z, Wang C. Introduction of electrospinning. In: *One-Dimensional Nanostructures. Electrospinning Technique and Unique Nanofibers*. Springer Briefs in Materials. Berlin: Springer; 2013. pp. 1-13. DOI: 10.1007/978-3-642-36427-3\_1
- [88] Yang X, Wang J, Guo H, Liu L, Xu W, Duan G. Structural design toward functional materials by electrospinning: A review. *e-Polymers*. 2020;**20**:682-712. DOI: 10.1515/epoly-2020-0068

- [89] Wang C, Wang J, Zeng L, Qiao Z, Liu X, Liu H, et al. Fabrication of electrospun polymer nanofibers with diverse morphologies. *Molecules*. 2019;**24**:834. DOI: 10.3390/molecules24050834
- [90] Xue J, Wu T, Dai Y, Xia Y. Electrospinning and electrospun nanofibers: Methods, materials and applications. *Chemical Reviews*. 2019;**119**:5298-5415. DOI: 10.1021/acs.chemrev.8b00593
- [91] Al-Hazeem NZA. Nanofibers and electrospinning method. In: Zykas GZ, Mitropoulos AC, editors. *Novel Nanomaterials: Synthesis and Applications*. London: IntechOpen; 2018. pp. 191-210. DOI: 10.5772/intechopen.72060
- [92] Williams GR, Raimi-Abraham BT, Luo CJ. Electrospinning fundamentals. In: *Nanofibers in Drug-Delivery*. London: UCL Press; 2018. pp. 24-59. DOI: 10.2307/j.ctv550dd1.6
- [93] Li Z, Wang C. Effects of working parameters on electrospinning. In: *One-Dimensional Nanostructures. Electrospinning Technique and Unique Nanofibers*. Springer Briefs in Materials. Berlin: Springer; 2013. pp. 15-28. DOI: 10.1007/978-3-642-36427-3\_2
- [94] Bhardwaj N, Kundu SC. Electrospinning: A fascinating fiber fabrication technique. *Biotechnology Advances*. 2010;**28**:325-347. DOI: 10.1016/j.biotechadv.2010.01.004
- [95] Korotcenkov G. Electrospun metal oxide nanofibers and their conductometric gas sensor application. Part 1: Nanofibers and features of their forming. *Nanomaterials*. 2021;**11**:1544. DOI: 10.3390/nano11061544
- [96] Esfahani H, Jose R, Ramakrishna S. Electrospun ceramic nanofiber mats today: Synthesis, properties, and applications. *Materials*. 2017;**10**:1238. DOI: 10.3390/ma10111238
- [97] Xia X, Dong XJ, Wei QF, Cai YB, Lu KY. Formation mechanism of porous hollow SnO<sub>2</sub> nanofibers prepared by one-step electrospinning. *eXPRESS Polymer Letters*. 2012;**6**(2):169-176. DOI: 10.3144/expresspolymlett.2012.18
- [98] Korotcenkov G. Electrospun metal oxide nanofibers and their conductometric gas sensor application. Part 2: Gas sensors and their advantages and limitations. *Nanomaterials*. 2021;**11**:1555. DOI: 10.3390/nano11061555
- [99] Deng Y. Semiconducting metal oxides: Morphology and sensing performance. In: *Semiconducting Metal Oxides for Gas Sensing*. Singapore: Springer Nature; 2019. pp. 53-75. DOI: 10.1007/978-981-13-5853-1
- [100] Wang C, Yin L, Zhang L, Xiang D, Gao R. Metal oxide gas sensors: Sensitivity and influencing factors. *Sensors*. 2010;**10**:2088-2106. DOI: 10.3390/s100302088
- [101] Katoch A, Abideen ZU, Kim J-H, Kim SS. Influence of hollowness variation on the gas-sensing properties of ZnO hollow nanofibers. *Sensors and Actuators B*. 2016;**232**:98-704. DOI: 10.1016/j.snb.2016.04.013
- [102] Katoch A, Choi S-W, Kim SS. Nanograins in electrospun oxide nanofibers. *Metals and Materials International*. 2015;**21**(2):213-221. DOI: 10.1007/s12540-015-4319-8
- [103] Katoch A, Sun G-J, Choi S-W, Byun J-H, Kim SS. Competitive influence of grain size and crystallinity on gas sensing performances of ZnO nanofibers. *Sensors and Actuators B*. 2013;**185**:411-416. DOI: 10.1016/j.snb.2013.05.030
- [104] Wal RL, Hunter GW, Xu JC, Kulis MJ, Berger GM, Ticich TM. Metal-oxide nanostructure and gas-sensing performance. *Sensors and*

- Actuators B. 2009;**138**:113-119.  
DOI: 10.1016/j.snb.2009.02.020
- [105] Comini E. Metal-oxide nanocrystals for gas sensing. *Analytical Chimica Acta*. 2006;**568**:28-40.  
DOI: 10.1016/j.aca.2005.10.069
- [106] Rothschild A, Komem Y. On the relationship between the grain size and gas-sensitivity of chemo-resistive metal-oxide gas sensors with nanosized grains. *Journal of Electroceramics*. 2004;**13**:97-301. DOI: 10.1007/s10832-004-5178-8
- [107] Rothschild A, Komem Y. The effect of grain size on the sensitivity of nanocrystalline metal-oxide gas sensors. *Journal of Applied Physics*. 2004;**95**:6374-6380. DOI: 10.1063/1.1728314
- [108] Liao Y, Fukuda T, Wang S. Electrospun metal oxide nanofibers and their energy applications. In: Rahman MM, Asiri AM, editors. *Nanofiber Research—Reaching New Heights*. London: IntechOpen; 2016. pp. 169-190. DOI: 10.5772/63414
- [109] Du H, Yang W, Sun Y, Yu N, Wang J. Oxygen-plasma-assisted enhanced acetone-sensing properties of ZnO nanofibers by electrospinning. *ACS Applied Materials & Interfaces*. 2020;**12**:23084-23093. DOI: 10.1021/acsami.0c03498
- [110] Zhang Y, Li J, An G, He X. Highly porous SnO<sub>2</sub> fibers by electrospinning and oxygen plasma etching and its ethanol sensing properties. *Sensors and Actuators B*. 2010;**144**:43-48.  
DOI: 10.1016/j.snb.2009.10.012s
- [111] Islam M, Srivastava AK, Basavaraja BM, Sharma A. “Nano-on-micro” approach enables synthesis of ZnO nano-cactus for gas sensing applications. *Sensors International*. 2021;**2**:100084. DOI: 10.1016/j.sint.2021.100084
- [112] Tomic M, Setka M, Vojkukva L, Vallejos S. VOCs sensing by metal oxides, conductive polymers, and carbon-based materials. *Nanomaterials*. 2021;**11**:552. DOI: 10.3390/nano11020552
- [113] Palgrave RG, Parkin IP. Aerosol assisted chemical vapor deposition using nanoparticle precursors: A route to nanocomposite thin films. *Journal of the American Chemical Society*. 2006;**128**(5):1587-1597. DOI: 10.1021/ja055563v
- [114] Andre RS, Mattoso LHC, Correa DS. Electrospun ceramic nanofibers and hybrid-nanofiber composites for gas sensing. *ACS Applied Nano Materials*. 2019;**2**:4026-4042. DOI: 10.1021/acsanm.9b01176
- [115] Imran M, Motta N, Shafiei M. Electrospun one-dimensional nanostructures: A new horizon for gas sensing materials. *Beilstein Journal of Nanotechnology*. 2018;**9**:2128-2170. DOI: 10.3762/bjnano.9.202
- [116] Abideen ZU, Kim J-H, Lee J-H, Kim J-Y, Mirzaei A, Kim HW, et al. Electrospun metal oxide composite nanofibers gas sensors: A review. *Journal of the Korean Ceramic Society*. 2017;**54**(5):366-379. DOI: 10.4191/kcers.2017.54.5.12
- [117] Xia Y, Li R, Chen R, Wang J, Xiang L. 3D architecture graphene/metal oxide hybrids for gas sensors: A review. *Sensors*. 2018;**18**:1456. DOI: 10.3390/s18051456
- [118] Mahji SM, Mirzaei A, Kim HW, Lim SS. Reduced graphene oxide (rGO)-loaded metal-oxide nanofiber gas sensors: An overview. *Sensors*. 2021;**21**:1352. DOI: 10.3390/s211041352
- [119] Gao Y, Zhang B, Cheng M, Zhao L, Lu G. P2GS.9—Gas sensors based on metal oxides decorated by reduced graphene oxide with enhanced gas sensing properties. In: *Proceedings of the*

17th International Meeting on Chemical Sensors (IMCS 2018); 15-19 July 2018; Vienna. Berlin: AMA Association for Sensors and Measurement; 2018. pp. 786-787. DOI: 10.5162/IMCS2018/P2GS.9

[120] Tuscharoen S, Hicheeranun W, Chananonawathorn C, Horprathum M, Kaewkhao J. Effect of sputtered pressure on Au nanoparticles formation decorated ZnO nanowire arrays. *Materials Today: Proceedings*. 2021;**43**:2624-2628. DOI: 10.1016/j.matpr.2020.04.626

[121] Annanouch FE, Haddi Z, Ling M, Di Maggio F, Vallejos S, Vilic T, et al. Aerosol-assisted CVD-grown PdO nanoparticle-decorated tungsten oxide nanoneedles extremely sensitive and selective to hydrogen. *ACS Applied Materials & Interfaces*. 2016;**8**(16): 10413-10421. DOI: 10.1021/acsami.6b00773

[122] Navarrete E, Llobet E. Synthesis of p-n heterojunctions via aerosol assisted chemical vapor deposition to enhance the gas sensing properties of tungsten trioxide nanowires: A mini-review. *Journal of Nanoscience and Nanotechnology*. 2021;**21**(4):2462-2471. DOI: 10.1166/jnn.2021.19105

[123] Tomic M, Setka M, Chmela O, Gràcia I, Figueras E, Cané C, et al. Cerium oxide-tungsten oxide core-shell nanowire-based microsensors sensitive to acetone. *Biosensors*. 2018;**8**(4): 116. DOI: 10.3390/bios8040116

[124] Choi MS, Mirzaei A, Na HG, Kim S, Kim DE, Lee KH, et al. Facile and fast decoration of SnO<sub>2</sub> nanowires with Pd embedded SnO<sub>2-x</sub> nanoparticles for selective NO<sub>2</sub> gas sensing. *Sensors and Actuators B*. 2021;**340**:129984. DOI: 10.1016/j.snb.2021.129984

[125] SnO<sub>2</sub> nanowires decorated by insulating amorphous carbon layers for improved room-temperature NO<sub>2</sub> sensing. *Sensors and Actuators B*.

2021;**326**:128801. DOI: 10.1016/j.snb.2020.128801

[126] Feng Y, Cho IS, Rao PM, Cai L, Zheng X. Sol-flame synthesis: A general strategy to decorate nanowires with metal oxide/noble metal nanoparticles. *Nano Letters*. 2013;**13**(3):855-860. DOI: 10.1021/nl300060b

[127] Vallejos S, Stoycheva T, Umek P, Navio C, Snyders R, Bittencourt C, et al. Au nanoparticle-functionalized WO<sub>3</sub> nanoneedles and their application in high sensitivity gas sensor devices. *Chemical Communications*. 2011;**47**: 565-567. DOI: 10.1039/C0CC02398A

[128] Vallejos S, Umek P, Stoycheva T, Annanouch F, Llobet E, Correig X, et al. Single-step deposition of Au- and Pt- nanoparticle-functionalized tungsten oxide nanoneedles synthesized via aerosol-assisted CVD, and used for fabrication of selective gas microsensors arrays. *Advanced Functional Materials*. 2013;**23**(10):1313-1322. DOI: 10.1002/adfm.201201871

[129] Vallejos S, Gràcia I, Figueras E, Cané C. Nanoscale heterostructures based on Fe<sub>2</sub>O<sub>3</sub>@WO<sub>3-x</sub> nanoneedles and their direct integration into flexible transducing platforms for toluene sensing. *ACS Applied Materials & Interfaces*. 2015;**7**(33):18638-18649. DOI: 10.1021/acsami.5b05081

[130] Shao H, Huang M, Fu H, Wang S, Wang L, Lu J, et al. Hollow WO<sub>3</sub>/SnO<sub>2</sub> hetero-nanofibers. Controlled synthesis and high efficiency of acetone vapor detection. *Frontiers in Chemistry*. 2019;**7**:785. DOI: 10.3389/fchem.2019.00785

[131] Lu Z, Zhou Q, Wang C, Wei Z, Xu L, Gui Y. Electrospun ZnO-SnO<sub>2</sub> composite nanofibers and enhanced sensing properties to SF<sub>6</sub> decomposition byproduct H<sub>2</sub>S. *Frontiers in Chemistry*. 2018;**6**:540. DOI: 10.3389/fchem.2018.00540

- [132] Lee J-H, Kim J-Y, Mirzaei A, Kim HW, Kim SS. Significant enhancement of hydrogen-sensing properties of ZnO nanofibers through NiO loading. *Nanomaterials*. 2018;**8**:902. DOI: 10.3390/nano8110902
- [133] Yan C, Lu H, Gao J, Zhu G, Yin F, Yang Z, et al. Synthesis of porous NiO-In<sub>2</sub>O<sub>3</sub> composite nanofibers by electrospinning and their highly enhanced gas sensing properties. *Journal of Alloys and Compounds*. 2017;**699**:567-574. DOI: 10.1016/j.jallcom.2016.12.307
- [134] Yousefzadeh M, Ghasemkhah F. Design of porous, core-shell, and hollow nanofibers. In: Barhoum A, Bechelany M, Makhlof ASH, editors. *Handbook of Nanofibers. Part I: Fundamental Aspects, Experimental Setup, Synthesis, Properties and Characterization*. 1st ed. Switzerland: Springer Nature; 2019. pp. 157-214. DOI: 10.1007/978-3-319-53655-2\_9
- [135] Vijayan P, Al-Maadeed M. Self-repairing composites for corrosion protection: A Review on recent strategies and evaluation methods. *Materials*. 2019;**12**:2754. DOI: 10.3390/ma12172754
- [136] Li F, Gao X, Wang R, Zhang T. Design of WO<sub>3</sub>-SnO<sub>2</sub> core-shell nanofibers and their enhanced gas sensing performance based on different work function. *Applied Surface Science*. 2018;**442**:30-37. DOI: 10.1016/j.apsusc.2018.02.122
- [137] Li F, Gao X, Wang R, Zhang T, Lu G. Study on TiO<sub>2</sub>-SnO<sub>2</sub> core-shell heterostructure nanofibers with different work function and its application in gas sensor. *Sensors and Actuators B*. 2017;**248**:812-819. DOI: 10.1016/j.snb.2016.12.009
- [138] Li F, Gao X, Wang R, Zhang T, Lu G, Barsan N. Design of core-shell heterostructure nanofibers with different work function and their sensing properties to trimethylamine. *ACS Applied Materials & Interfaces*. 2016;**8**:19799-19806. DOI: 10.1021/acsami.6b04063
- [139] Lee J-H, Katoch A, Choi S-W, Kun J-H, Kim HW, Kim SS. Extraordinary improvement of gas-sensing performances in SnO<sub>2</sub> nanofibers due to creation of local p-n heterojunctions by loading reduced graphene oxide nanosheets. *ACS Applied Materials & Interfaces*. 2015;**7**:3101-3109. DOI: 10.1021/am5071656
- [140] Dang TK, Son NT, Lanh NT, Phuoc PH, Viet NN, Thong LV, et al. Extraordinary H<sub>2</sub>S sensing performance of ZnO/rGO external and internal heterojunctions. *Journal of Alloys and Compounds*. 2021;**879**:160457. DOI: 10.1016/j.jallcom.2021.160457
- [141] Salehi T, Taherizadeh A, Bahrami A, Allafchian A, Ghafarinia. Toward a highly functional hybrid ZnO nanofiber-rGO gas sensor. *Advanced Engineering Materials*. 2020;**22**:202000005. DOI: 10.1002(adem.202000005
- [142] Masa S, Robés D, Hontañón E, Lozano J, Eqtesadi S, Narros A. Graphene-tin oxide composite nanofibers for low temperature detection of NO<sub>2</sub> and O<sub>3</sub>. *Sensors & Transducers*. 2020;**246**(7):71-78
- [143] Wang D, Tang M, Sun J. Direct fabrication of reduced graphene oxide@SnO<sub>2</sub> hollow nanofibers by single-capillary electrospinning as fast NO<sub>2</sub> gas sensor. *Journal of Nanomaterials*. 2019;**2019**:1929540. DOI: 10.1155/2019/1929540
- [144] Li W-T, Zhang X-D, Guo X. Electrospun Ni-doped SnO<sub>2</sub> nanofiber array for selective sensing of NO<sub>2</sub>. *Sensors and Actuators B*. 2017;**244**:509-521. DOI: 10.1016/j.snb.2017.01.022
- [145] Park S, Bulemo PM, Koo W-T, Ko J, Kim I-D. Chemiresistive acetylene

- sensor fabricated from Ga-doped ZnO nanofibers functionalized with Pt catalysts. *Sensors and Actuators B*. 2021;**343**:130137. DOI: 10.1016/j.snb.2021.130137
- [146] Lalwani SK, Beniwal A, Sunny. Enhancing room temperature ethanol sensing using electrospun Ag-doped SnO<sub>2</sub>-ZnO nanofibers. *Journal of Materials Science: Materials in Electronics*. 2020;**31**:17212-17224. DOI: 10.1007/s10854-020-04276-9
- [147] Abideen ZU, Kim J-H, Mirzaei A, Kim HW, Kim SS. Sensing behavior to ppm-level gases and synergistic sensing mechanism in metal-functionalized rGO-loaded ZnO nanofibers. *Sensors and Actuators B*. 2018;**255**:1884-1896. DOI: 10.1016/j.snb.2017.08.210
- [148] Al-Dhahebi AM, Gopinath SCB, Saheed MSM. Graphene impregnated electrospun nanofiber sensing materials: A comprehensive overview on bridging laboratory set-up to industry. *Nano Convergence*. 2020;**2**:27. DOI: 10.1186/s4080-020-00237-4
- [149] Chen C, Tang Y, Vlahovic B, Yan F. Electrospun polymer nanofibers decorated with noble metal nanoparticles for chemical sensing. *Nanoscale Research Letters*. 2017;**12**:451. DOI: 10.1186/s11671-017-2216-4
- [150] Yang T, Zhan L, Huan CZ. Recent insights into functionalized electrospun nanofibrous films for chemo-/bio-sensors. *Trends in Analytical Chemistry*. 2020;**124**:115813. DOI: 10.1016/j.trac.2020.115813
- [151] Kim J-H, Abideen ZU, Zheng Y, Kim SS. Improvement of toluene-sensing performance of SnO<sub>2</sub> nanofibers by Pt functionalization. *Sensors*. 2016;**16**:1857. DOI: 10.3390/s16111857
- [152] Kim S, Brady J, Al-Badani F, Yu S, Hart J, Jung S, et al. Nanoengineering approaches toward artificial nose. *Frontiers in Chemistry*. 2021;**9**:629329. DOI: 10.3389/fchem.2021.629329
- [153] Hierlemann A. CMOS-based chemical sensors. In: Brand O, Fedder GK, editors. *Advanced Micro and Nanosystems*. Vol. 2. CMOS-MEMS. 1st ed. Weinheim: Wiley-VCH; 2005. p. 335-390. DOI: 10.1002/9783527616718.ch7
- [154] Gao W, Ota H, Kiriya D, Takei K, Javey A. Flexible electronics toward wearable sensing. *Accounts of Chemical Research*. 2019;**52**:523-533. DOI: 10.1021/acs.accounts.8b00500
- [155] Hung CM, Thanh DTT, Van Hieu N. On-chip growth of semiconductor metal oxide nanowires for gas sensors. A review. *Journal of Science: Advanced Materials and Devices*. 2017;**2**:263-285. DOI: 10.1016/j.jsadm.2017.07.009
- [156] Yang D, Cho I, Kim D, Lim MA, Li Z, Ok JG, et al. Gas sensor by direct growth and functionalization of metal oxide/metal sulfide core-shell nanowires onto flexible substrates. *ACS Applied Materials & Interfaces*. 2019;**11**:24298-24307. DOI: 10.1021/acsami.9b06951
- [157] XiaoQi Z, HuanYu C. Flexible and stretchable metal oxide gas sensors for healthcare. *Science China Technological Sciences*. 2019;**62**:209-223. DOI: 10.1007/s11431-018-9397-5
- [158] Habibi M, Ahmadian-Yazdi M-R, Eslamian M. Optimization of spray coating for the fabrication of sequentially deposited planar perovskite solar cells. *Journal of Photonics for Energy*. 2017;**7**(2):022003. DOI: 10.1117/1.JPE.7.022003
- [159] Li Y, Delaunay J-J. Progress toward nanowire device assembly technology. In: Prete P, editor. *Nanowires*. London: IntechOpen; 2010. 25 pp. DOI: 10.5772/39521

- [160] Freer EM, Grachev O, Duan X, Martín S, Stumbo DP. High-yield self-limiting single-nanowire assembly with dielectrophoresis. *Nature Nanotechnology*. 2010;**5**:525-530. DOI: 10.1038/NNANO.2010.206
- [161] Chmela O, Sadílek J, Domènech-Gil G, Samà J, Somer J, Mohan R, et al. Selectively arranged single-wire based nanosensor array systems for gas monitoring. *Nanoscale*. 2018;**10**:9087-9096. DOI: 10.1039/c8nr01588k
- [162] Yuan H, Zhou Q, Zhang Y. Improving fiber alignment during electrospinning. In: Afshari M, editor. *Electrospun Nanofibers*. Woodhead Publishing Series in Textiles. Amsterdam: Elsevier; 2017. pp. 125-147. DOI: 10.1016/B978-0-08-100907-9.00006-4
- [163] Prabhakaran MP, Vatankhah E, Ramakrishna S. Electrospun aligned PHBV/collagen nanofibers as substrates for nerve tissue engineering. *Biotechnology and Bioengineering*. 2013;**110**(10):2775-2784. DOI: 10.1002/bit.24937
- [164] Munir MW, Ali U. Classification of electrospinning methods. In: Ghamsari MS, Dhara S, editors. *Nanorods and Nanocomposites*. London: IntechOpen; 2020. 19 pp. DOI: 10.5772/intechopen.88654
- [165] Li D, Ouyang G, McCann JT, Xia Y. Collecting electrospun nanofibers with patterned electrodes. *Nano Letters*. 2005;**5**(5):913-916. DOI: 10.1021/nl0504235
- [166] Li D, Wang Y, Xia Y. Electrospinning nanofibers as uniaxially aligned arrays and layer-by-layer stacked films. *Advanced Materials*. 2004;**18**(4):361-366. DOI: 10.1002/adma.200306226
- [167] Li D, Wang Y, Xia Y. Electrospinning of polymeric and ceramic nanofibers as uniaxially aligned arrays. *Nano Letters*. 2003;**3**(8):1167-1171. DOI: 10.1021/nl0344256
- [168] Meng Y, Liu G, Liu A, Guo Z, Sun W, Shan F. Photochemical activation of electrospun  $\text{In}_2\text{O}_3$  nanofibers for high performance electronic devices. *ACS Applied Materials & Interfaces*. 2017;**9**:10805-10812. DOI: 10.1021/acsami.6b15916
- [169] Kim I-D, Jeon E-K, Choi S-H, Choi D-K, Tuller HL. Electrospun  $\text{SnO}_2$  nanofiber mats with thermo-compression step for gas sensing applications. *Journal of Electroceramics*. 2010;**25**:159-167. DOI: 10.1007/s10832-010-9607-6
- [170] Yang D-J, Kamienchik I, Youn DY, Rothschild A, Kim I-D. Ultrasensitive and highly selective gas sensor based on electrospun  $\text{SnO}_2$  nanofibers modified by Pd loading. *Advanced Functional Materials*. 2010;**20**:4258-4264. DOI: 10.1002/adfm.201001251
- [171] Cui Y, Meng Y, Wang Z, Wang C, Liu G, Martins R, et al. High performance electronic devices based on nanofibers via a crosslinking welding process. *Nanoscale*. 2018;**10**:19427-19434. DOI: 10.1039/c8nr05420g
- [172] Park J-U, Hardy M, Kang SJ, Barton K, Adair K, Mukhopadhyay DK, et al. High-resolution electrohydrodynamic jet printing. *Nature Materials*. 2007;**6**:782-789. DOI: 10.1038/nmat1974
- [173] Zou W, Yu H, Zhou P, Liu L. Tip-assisted electrohydrodynamic jet printing for high resolution microdroplet deposition. *Materials and Design*. 2019;**185**:107609. DOI: 10.1016/j.matdes.2019.107609
- [174] Liang Y, Yong J, Yu Y, Nirmalathas A, Ganesan K, Evans R, et al. Direct electrohydrodynamic patterning of high-performance all metal oxide thin-film electronics. *ACS Nano*.

2019;**13**:13957-13964. DOI: 10.1021/acs.nano.9b05715

[175] Wu H, Yu J, Cao R, Yang Y, Tang Z. Electrohydrodynamic inkjet printing of Pd loaded SnO<sub>2</sub> nanofibers on a CMOS micro hotplate for low power H<sub>2</sub> detection. *AIP Advances*. 2018;**8**:055307. DOI: 10.1063/1.5029283

[176] Kang K, Yang D, Park J, Kim S, Cho I, Yang H-H, et al. Micropatterning of metal oxide nanofibers by electrohydrodynamic (EHD) printing towards highly integrated and multiplexed gas sensor applications. *Sensors and Actuators B*. 2017;**250**:574-583. DOI: 10.1016/j.snb.2017.04.194

[177] Schmidt V, Riel H, Senz S, Karg S, Riess W, Gösele U. Realization of a silicon nanowire vertical surround-gate field-effect transistor. *Small*. 2006;**2**(1):85-88. DOI: 10.1002/sml.200500181

[178] Ng HT, Han J, Yamada T, Nguyen P, Chen YP, Meyyappan M. Single crystal nanowire vertical surround-gate field-effect transistor. *Nano Letters*. 2004;**4**(7):1247-1252. DOI: 10.1021/nl049461z

[179] Fan HJ, Werner P, Zacharia M. Semiconductor nanowires: From self-organization to patterned growth. *Small*. 2006;**2**(6):700-717. DOI: 10.1002/sml.200500495

[180] Zhang B, Gao P-X. Metal oxide nanoarrays for chemical sensing: A review of fabrication methods, sensing modes, and their inter-correlations. *Frontiers in Materials*. 2019;**6**:65. DOI: 10.3389/fmats.2019.00055

[181] Mkhize N, Murugappan K, Castell MR, Bhaskaran H. Electrohydrodynamic jet printed conducting polymer for enhanced chemiresistive gas sensors. *Journal of Materials Chemistry C*. 2021;**9**:4591-4596. DOI: 10.1039/d0tc05719c

[182] Zhang Z, He H, Fu W, Ji D, Ramakrishna S. Electro-hydrodynamic direct-writing technology toward patterned ultra-thin fibers: Advances, materials and applications. *Nano Today*. 2020;**35**:100942. DOI: 10.1016/j.nantod.2020.100942

[183] Xu W, Zhang S, Xu W. Recent progress on electrohydrodynamic nanowire writing. *Science China Materials*. 2019;**62**(11):1709-1726. DOI: 10.1007/s40483-019-9583-5

[184] He X-X, Zheng J, Yu G-F, You M-H, Yu M, Ning X, et al. Near-field electrospinning: Progress and applications. *The Journal of Physical Chemistry*. 2017;**121**:8663-8678. DOI: 10.1021/acs.jpcc.6b12783

[185] Huang Y, Bu N, Duan Y, Pan Y, Liu H, Yin Z, et al. Electrohydrodynamic direct-writing. *Nanoscale*. 2013;**5**:12007-12017. DOI: 10.1039/c3nr04329k

[186] Sun D, Chang C, Sha L, Lin L. Near-field electrospinning. *Nano Letters*. 2006;**6**(4):839-842. DOI: 10.1021/nl0602701

[187] Lim K, Jo Y-M, Yoon J-W, Lee J-H. Metal oxide patterns of one-dimensional nanofibers: On-demand, direct-write fabrication, and application as a novel platform for gas detection. *Journal of Materials Chemistry A*. 2019;**7**:24919-24928. DOI: 10.1039/c9ta09708b

[188] Ruggieri F, Di Camillo D, Lozzi L, Santucci S, De Marcellis A, Ferri G, et al. Preparation of nitrogen doped TiO<sub>2</sub> nanofibers by near field electrospinning (NFES) technique for NO<sub>2</sub> sensing. *Sensors and Actuators B*. 2013;**179**:107-113. DOI: 10.1016/j.snb.2012.10.094

[189] Wang X, Zheng G, He G, Wei J, Liu H, Lin Y, et al. Electrohydrodynamic direct-writing ZnO nanofibers for device applications. *Materials Letters*. 2013;**109**:58-61. DOI: 10.1016/j.matlet.2013.07.051